CASL-U-2012-0037-000

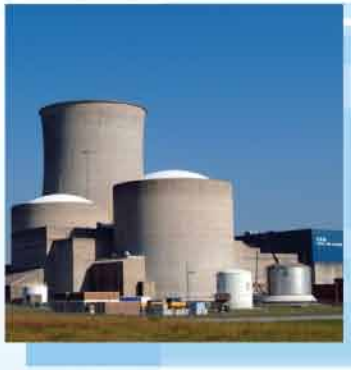

Power uprates
and plant life extension

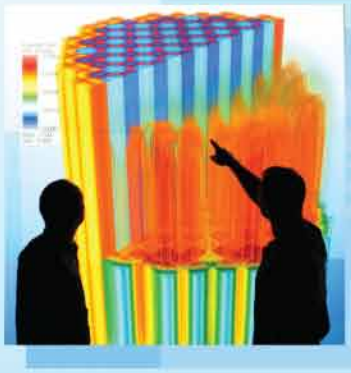

Engineering design
and analysis

Science-enabling
high performance
computing

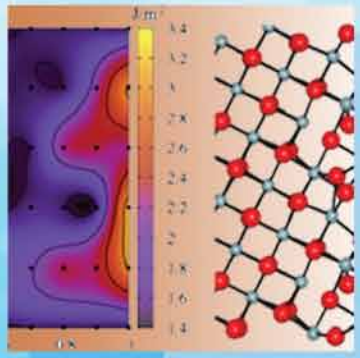

Fundamental science

Plant operational data

Consortium for Advanced Simulation of LWRs

Thermal Hydraulic Validation Report

CASL Mile Stone: L3:AMA.VAL.P4.02

Authors: J. Yan, P. Yuan, Y. Xu, Zeses Karoutas

Westinghouse Electric Company

Emilio Popov, Sreekanth Pannala, Alan Stagg

Oak Ridge National Lab

Scott Lucas, Hongbin Zhang

Idaho National Lab

Robert Brewster, Emilio Baglietto

CD-Adapco

Elvis Dominguez-Ontiveros, Yassin Hassan

Texas A&M

March 2012

U.S. DEPARTMENT OF ENERGY | Nuclear Energy

Please complete sections appropriate for this record.

a)REVISION LOG

Revision	Date	Affected Pages	Revision Description
0	3/29/2012		Original Issue

Document pages that are:

Export Controlled _____NO_____

IP/Proprietary/NDA Controlled_____NO_____

Sensitive Controlled_____NO_____

Requested Distribution:

To:

Copy:

EXECUTIVE SUMMARY

The current report is written to summarize the thermal hydraulic validation work for the CASL project. The objective of this activity is to benchmark Computational Fluid Dynamics (CFD) analyses with available data for different flow conditions.

Four validation cases have been performed:

Case 1: Turbulent Pipe Flow. (ORNL)
Case 2: Turbulent Flow in a U-bent Channel. (ORNL)
Case 3: Flow in a 5 × 5 Rod Bundle with Spacer-Grids. (WEC)
Case 4: Flow Passing Through a Heated Rod Bundle. (INL)

The detailed case setup and comparison between CFD results and available data are presented here.

Validation Case 1: Turbulent Pipe Flow

OBJECTIVES

The test is a classical example of gas flow in a round pipe. It tests the ability of the code to compute the velocity profiles at different dominantly high Reynolds numbers Reynolds number K-E turbulence models are used and to that extent, the test evaluates the implementation of wall functions in the K-E models. References [1.1] and [1.2] give more insight on the investigated problem.

PROBLEM DESCRIPTION

The problem geometry is a pipe of diameter (D) = 129.36 ± 0.08 mm, and a length of 202×D mm. The experiments were performed in the Princeton/DARPA/ONR Superpipe (http://www.princeton.edu/~gasdyn/index.html#superpipe_data), a facility constructed to enable the study of fully developed turbulent pipe flow over a wide range of Reynolds numbers. The working fluid is air at ambient temperature with pressures up to 187 atmospheres, allowing variations in the kinematic viscosity to obtain Reynolds numbers in the range $Re_D = 31\times10^3 – 35\times10^6$. The maximum Mach number encountered in the facility is approximately 0.07 (the incompressible flow assumption is still valid). Depending on how the simulation is set up, one could alter the pipe diameter and air viscosity to run the simulation at the same Re_D.

KEY PARAMETER COMPARISONS: TURBULENT PIPE FLOW

The velocity profiles are taken at 10 m section from the pipe inlet. This is the calculated total length of the pipe as well. Y+ values are computed by extracting the wall distance from the code and using the Frictional velocity from the test. The Y+ in the test (horizontal axis) has values that go over the pipe centerline. Although, this causes some uncertainty in the method of calculating Y+ in the experiment, we will assume that the wall distance has been correctly determined.

CFD MODEL INFORMATION

b) Software and Version:

The engineering simulation software, STARCCM+, version 6.04.016 is used for the simulation, running on an amd64 eight core (double quad) 64GB RAM machine.

c) Solver:

Segregated steady flow. AMG V-cycle for pressure and turbulence and Flex cycle for velocity. Relaxation: Gauss-Seidel, acceleration for pressure – Conjugate Gradient.

d) Descretization Schemes used in the model

Second order convection was used for all properties.

e) Domain

The computational domain represents a cylinder (pipe) 10 m long. It is not visualized because of its simplicity. The sampled surface is at the exit plane.

f) Mesh information, cell type, cell count, meshing parameters

Only one mesh was used for all calculations. It is polyhedral stretched (elongated) along the main flow axis with a factor of 5. This technique saves memory and run time, because it reduces the overall cell count. The Polyhedral mesh information is summarized in Table 1.4-1. A mesh view is given in Figure 1.4-1.

Table 1.4-1 General mesh settings and total cell count for the Polyhedral mesh

Base size	5 mm
Automatic surface repair	Minimum proximity: 0.05 Minimum quality: 0.01
CAD projection	Yes
Prism layer	2
Prism layer thickness	33.3% of base
Surface curvature	36.0
Surface growth rate	1.3
Surface proximity	# Points in gap: 2.0; Search Floor: 0.0m
Surface size	Relative minimum size: 25% of base; Relative target size: 100% of base.
Mesh size	387,775 polyhedral cells

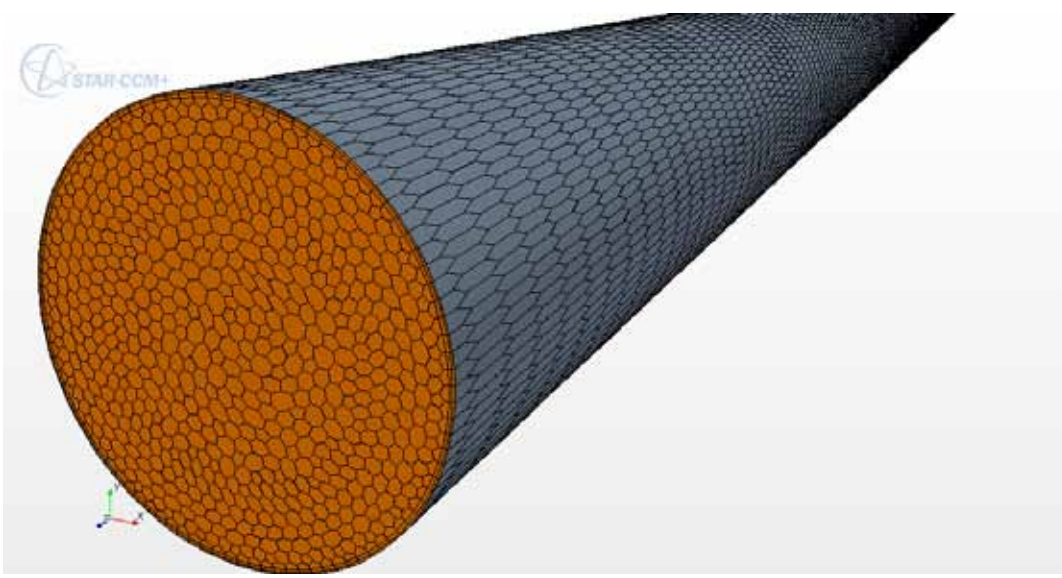

Figure 1.4-1 Pipe polyhedral mesh overall representation

g) Turbulence model

The default turbulence option, 'Realizable k-e Two-Layer and all y+ Wall Treatment' is used as a starting point for all Reynolds numbers. Once results were obtained, some other models were tested: the Standard k-e Low Re model(Re ~ 31,577) and the 'AKN Low Re' model (Re ~ 230,460) . For more information on these particular models refer to STARCCM+ User guide.

h) Fluid properties

Table 1.4-2 Fluid properties

Reynolds number	31, 577	230, 460	1, 023, 800
Reference Temperature (K)	3.0012E+02	2.9794E+02	2.9840E+02
Reference Pressure (Pa)	1.0029E+05	2.8739E+05	1.4882E+06
Density (kg/m^3)	1.1644E+00	3.3628E+00	1.7444E+01
Viscosity (Pa-s)	1.8487E-05	1.8408E-05	1.8601E-05

i) Boundary Conditions

The boundary conditions used in the model are listed in Table 1.4-3.

Table 1.4-3 Boundary conditions

Boundary Group	Location	Boundary Condition
Inlet	Inlet in Figure 4-1	Velocity inlet
Outlet	Exit in Figure 4-1	Pressure outlet (0 psig)
All others		No-slip wall

RESULTS & CONCLUSIONS

The calculations were run on a Linux server in serial mode (single core) due to the small mesh size. The solutions residuals for the three different Re numbers, using the default turbulence model (Realizable k-e two layer) are shown in Figure 1.5-1 through Figure 1.5-3. They show stable and low values for the monitored parameters.

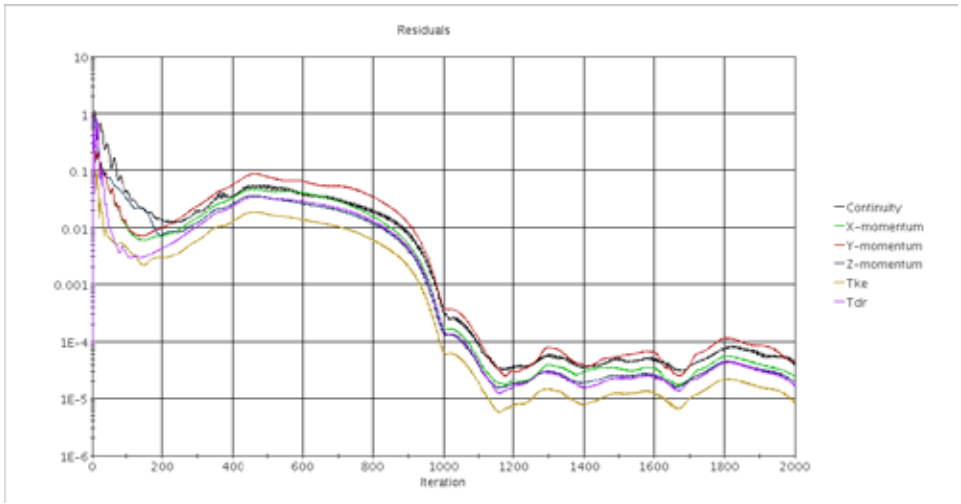

Figure 1.5-1 Residuals for Re = 31, 576 run

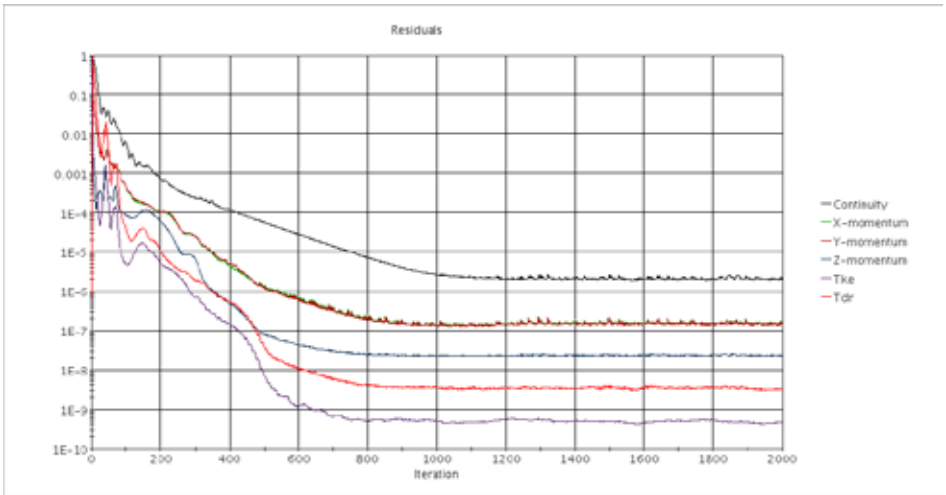

Figure 1.5-2 Residuals for Re = 203, 460 run

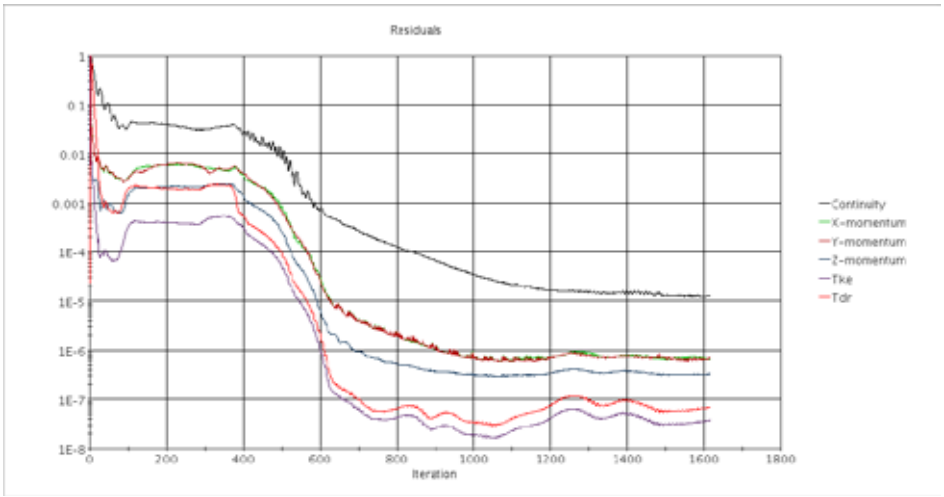

Figure 1.5-3 Residuals for Re = 1, 023, 800 run

In general, the results match very well with the test data for all Re numbers. The different k-e turbulence models give practically the same results. The predicted velocity is higher than the

measured in the bulk flow and is lower closer to the wall. This result is systematically repeated for all other models.

The Realizable k-e model (Default option in STARCCM+) matches better in the high Re flows. No other model was used for the highest Re of 1,023,800. Based on this result, the other two tests at lower Re were recalculated with Low Re k-e models. The test with Re = 31, 576 was repeated with the Standard k-e Low Re, while for the Re= 230, 460 test, the AKN Low Re k-e was used. Both attempts show improvement in the predictions away from the wall.

For the near wall region relative to mesh size, the viscous velocity might have been computed only for the lowest Re of 31, 576. The wall Y+ values for the other two Re numbers are quite high, and most likely the 'law of wall' has been applied. No any particular difference is seen in the velocity profile behavior next to the wall which confirms a valid application of the wall functions.

PLOT DATA

The velocities are plotted in Figure 1.6-1 through Figure 1.6-3, along with the test data. As mentioned above the test Y+ exceeds the pipe centerline which poses some questions on how the Y+ was calculated in the experiment. The distance to the wall for each cell was taken from the STARCCM+ mesh and the Y+ was computed with the frictional velocity from the test.

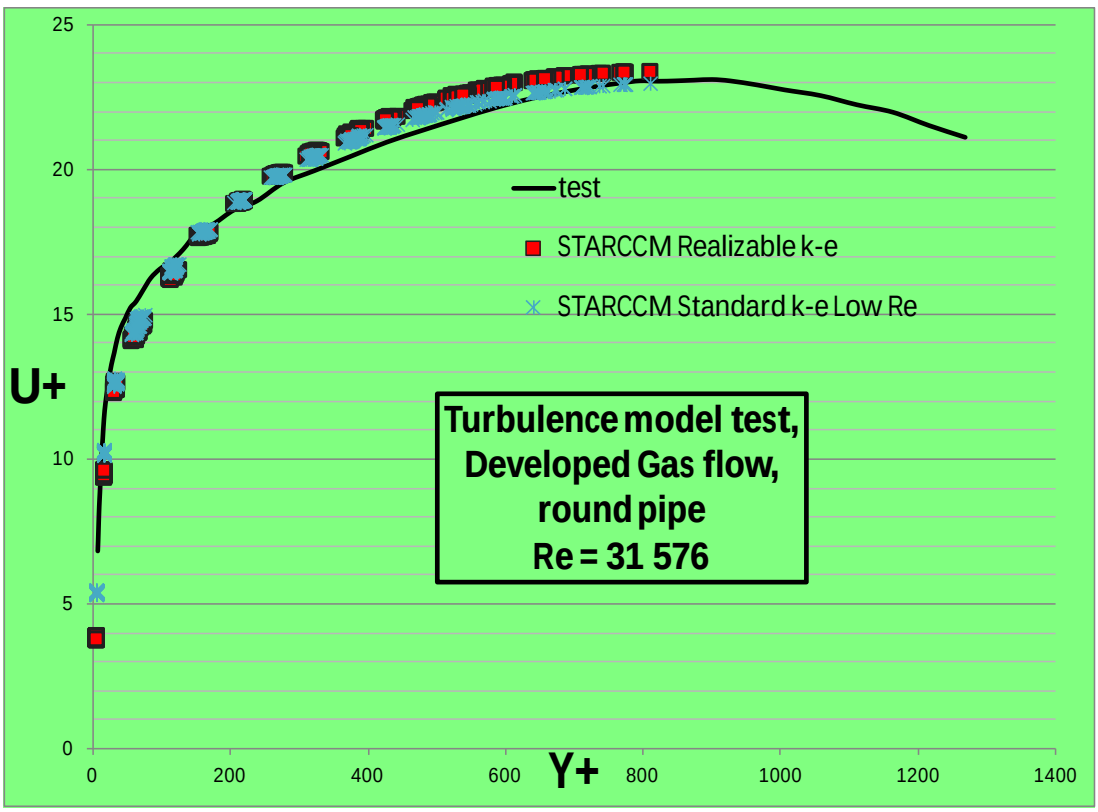

Figure 1.6-1 Re =31, 576 velocity results

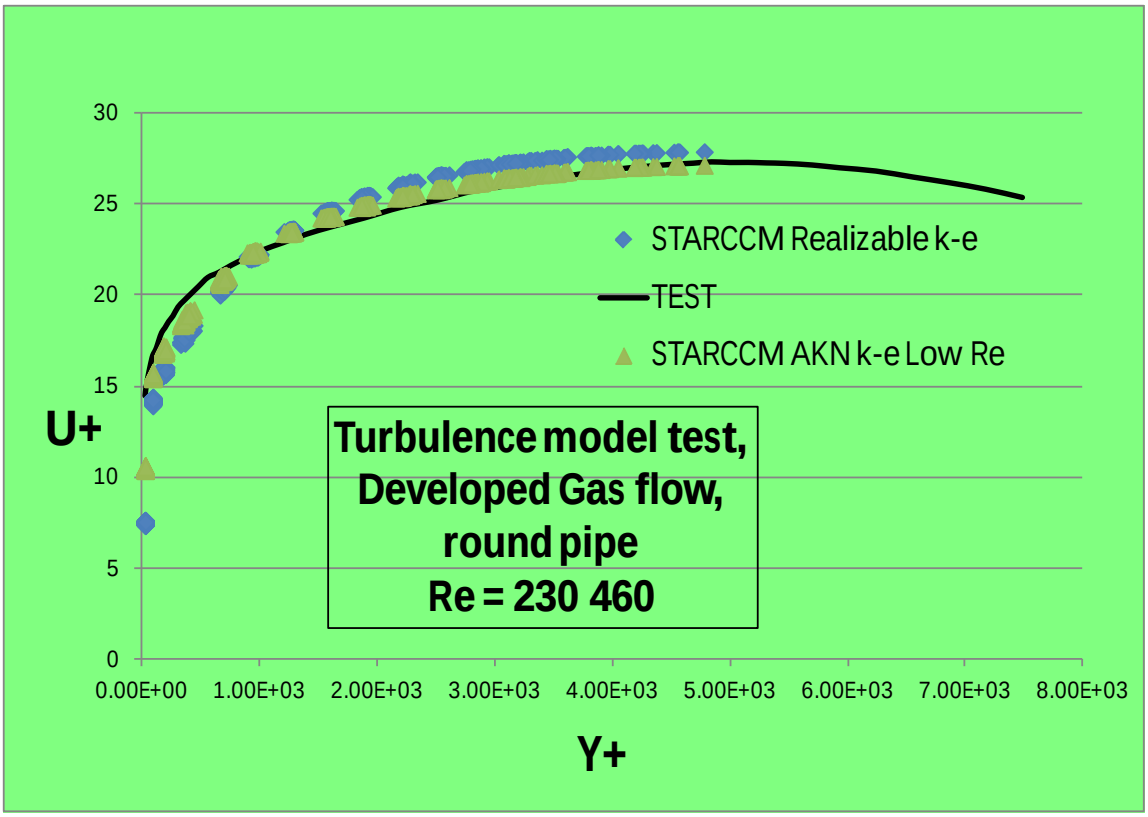

Figure 1.6-2 Re = 230, 460 velocity results

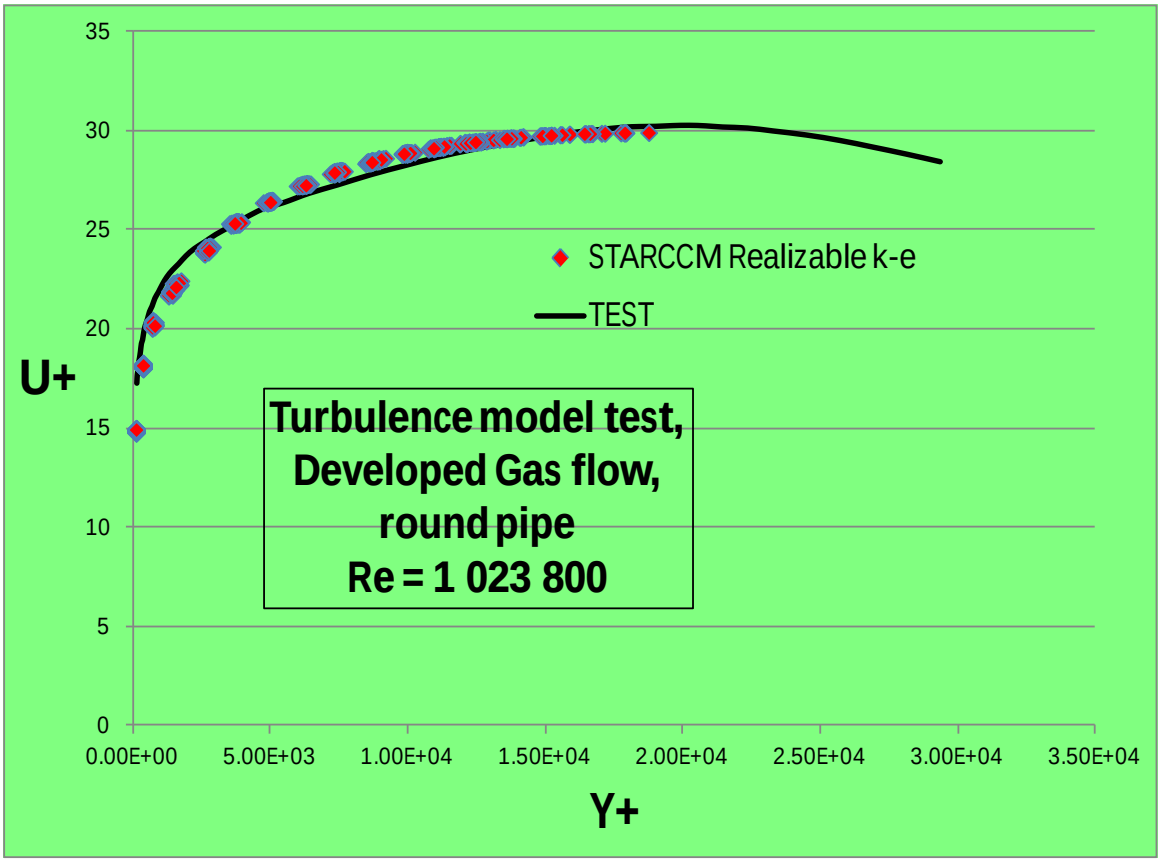

Figure 1.6-3 Re = 1, 023, 800 velocity results

REFERENCES

1. Zagarola, M. V. and A. J. Smits (1998). "Mean-flow scaling of turbulent pipe flow." Journal of Fluid Mechanics **373**: 33-79.
2. Zagarola, M. V. and A. J. Smits (1997). "Scaling of the Mean Velocity Profile for Turbulent Pipe Flow." Physical Review Letters **78**(2): 239-242.

Validation Case 2: Turbulent Flow in U-bent Channel

OBJECTIVES

Turbulent flow in confined, bent geometries is characteristic of flow in various nuclear reactor designs. This case tests the ability to capture secondary, cross-stream motions induced by the transverse pressure gradient as well as by the cross-stream, Reynolds stress gradients for turbulent, confined, single-phase flow in a curved duct. The experiment is described in [2.1] and [2.2].

PROBLEM DESCRIPTION

Water at 20°C flows into a duct bent at 180 degrees and of square cross section (4.45 × 4.45 cm^2) with an uncertainty of ±0.02 × 0.02 cm^2. The test section is composed of two straight tangent ducts and a bend (Figure 2.2-1). Both tangents are 31 hydraulic diameters long and attached to the 0° (inlet) and 180° (outlet) planes of the bend. The test section is part of a closed loop. A flow-straightening section of length 7.15 hydraulic diameters is placed upstream of the straight duct attached to the bend inlet to eliminate residual swirl and weak secondary motion and to accelerate the flow's stream-wise development as it approaches the bend. The ratio of the bend mean radius of curvature to hydraulic diameter is RcDH = 3.35. The measured flow rate corresponds to a Reynolds number of Re = 56,700 (bulk average velocity UB=1.28 m/s) and a Dean number of De = 21,900 through the bend.

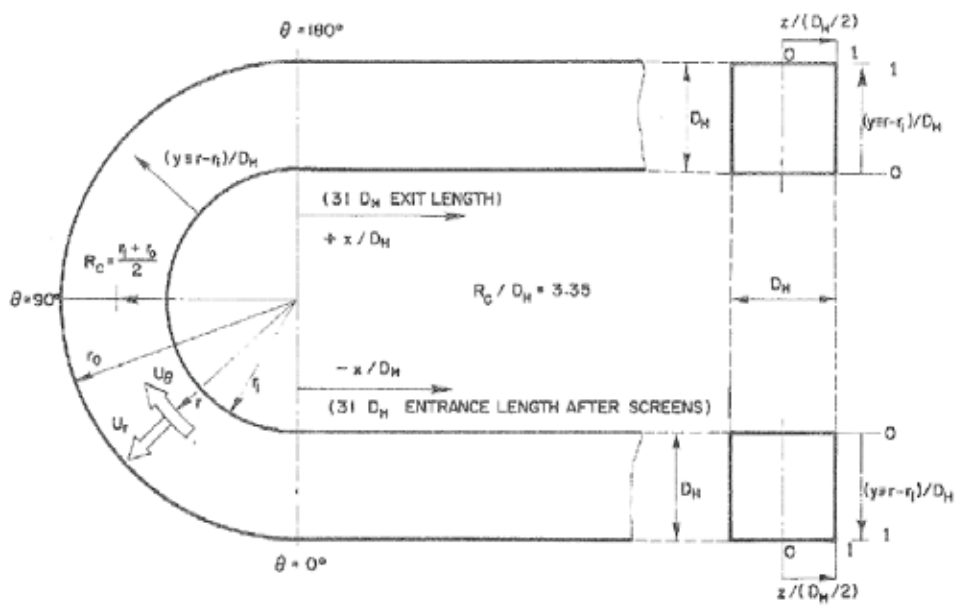

Figure 2.2-1 Schematic diagram of the U-bend test

KEY PARAMETER COMPARISONS: TURBULENT FLOW IN U-BENT CHANNEL

Comparisons to velocity data at two streamwise locations are requested:

1) at XH = -1 in the upstream tangent where influence of the bend has propagated via the pressure field, and
2) at θ = 90° at the halfway point in the bend
Data is provided in tabulated form for three positions inside the channel: at midplane (zero coordinate), half distance (0.50) between midplane and bottom/top, and half-half distance, or 0.75 from midplane to bottom/top. All coordinate are non-dimensional. The radial coordinate starts from '0' (inner channel side) to '1' (outer side). Around thirty velocity data points are taken for each position in two velocity directions: 'theta', or along the flow stream; and 'radial' – across the channel.

CFD MODEL INFORMATION

a) Software and Version:

STARCCM+ computer code is used for the simulation, version: 6.04.016, running on amd64 eight core (double quad) 64GB RAM machine.

b) Solver:

Segregated steady flow. AMG V-cycle for pressure and turbulence and Flex cycle for velocity. Relaxation: Gauss-Seidel, acceleration for pressure – Conjugate Gradient.

c) Descretization Schemes used in the model

Second order convection for all properties.

d) Domain (Picture)

The computing domain is shown in Figure 2.4-1. The upstream tangent is included in full. Both sampling locations are marked: -1X is positioned one hydraulic diameter before the bend entrance, and the 90 deg. sampling is at the middle of the bend.

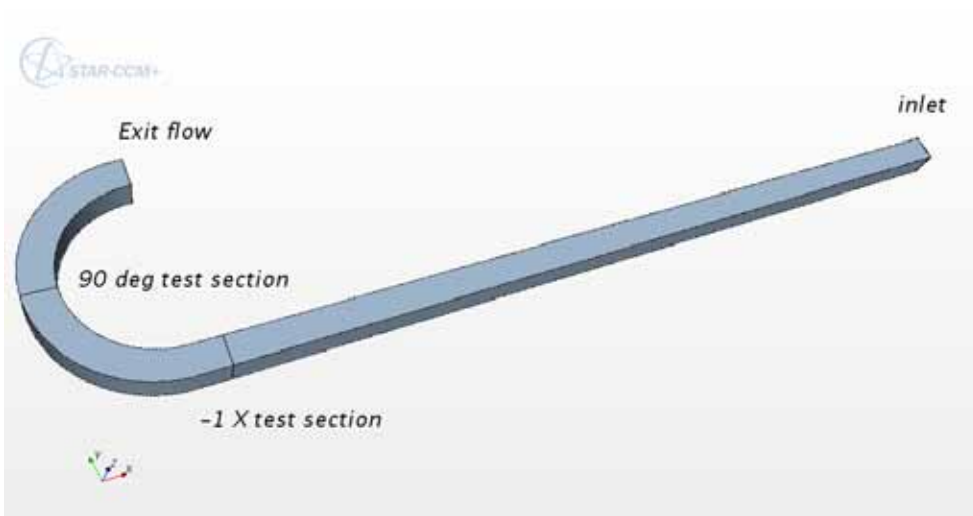

Figure 2.4-1 Computational domain

e) Mesh information, cell type, cell count, meshing parameters

Two types of meshes were generated: polyhedral, using the Thin mesher, and Trim, using the trim mesher. The Trim mesh has two modifications as described below.
The Polyhedral mesh information is summarized in Table 2.4-1. A mesh cross section is given in Figure 2.4-2.

Table 2.4-1 General mesh settings and total cell count for the Polyhedral mesh

Base size	10 mm
Automatic surface repair	Minimum proximity: 0.05 Minimum quality: 0.01
CAD projection	Yes
Maximum cell size	N/A
Prism layer	N/A
Prism layer thickness	N/A
Surface curvature	36.0
Surface growth rate	1.3
Surface proximity	# Points in gap: 2.0; Search Floor: 0.0m
Surface size	Relative minimum size: 10% of base; Relative target size: 10% of base.
Mesh size	1.86 million polyhedral cells

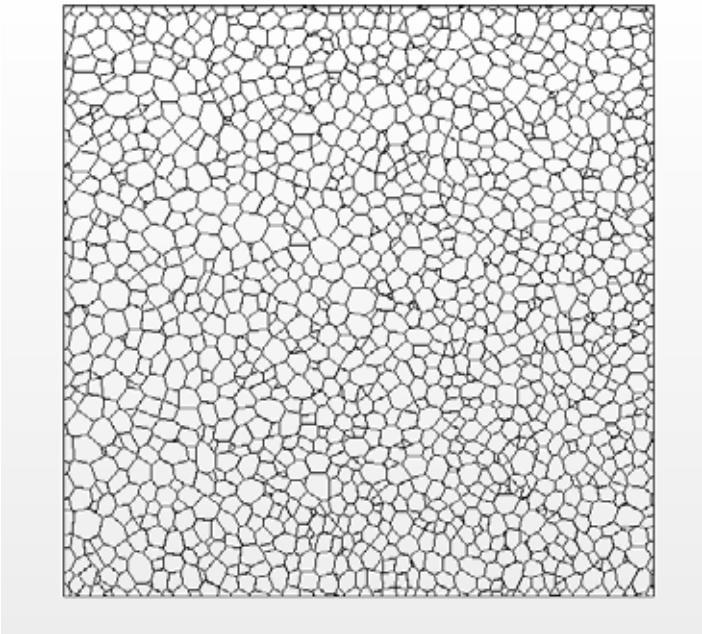

Figure 2.4-2 U bend polyhedral mesh sectional cut across the channel

Two different Trim meshes were developed. Their parameters and mesher setting are given in Table 2.4-2. The purpose for developing two meshes was that the first mesh (Mesh-1) had large cells in the central area and the obtained result was quite coarse. Then that area was refined, which resulted in the second mesh. This process tripled the overall cell count.

Table 2.4-2 General mesh settings and total cell count for the Trim meshes

Mesh name	Trim Mesh-1	Trim Mesh-2
Base size	10 mm	10 mm
Automatic surface repair	Minimum proximity: 0.05 Minimum quality: 0.01	Minimum proximity: 0.05 Minimum quality: 0.01
CAD projection	Yes	Yes
Maximum cell size	10,000	10
Prism layer	2	2
Prism layer thickness	33.3	33.3
Surface curvature	36.0	36.0
Surface growth rate	1.3	1.3
Surface proximity	# Points in gap: 2.0; Search Floor: 0.0m	# Points in gap: 2.0; Search Floor: 0.0m
Surface size	Relative minimum size: 10% of base; Relative target size: 10% of base.	Relative minimum size: 10% of base; Relative target size: 10% of base.
Mesh size	1.29 million cells total 12,103 tets 1,070,603 hexes 98,028 wedges 115,105 polyhedral 1,519 pyramid	3.48 million total 12.103 tets 3.335,143 hexes 98,028 wedges 36,301 polyherdal 1,519 pyramid

The meshes are shown in Figure 2.4-3.

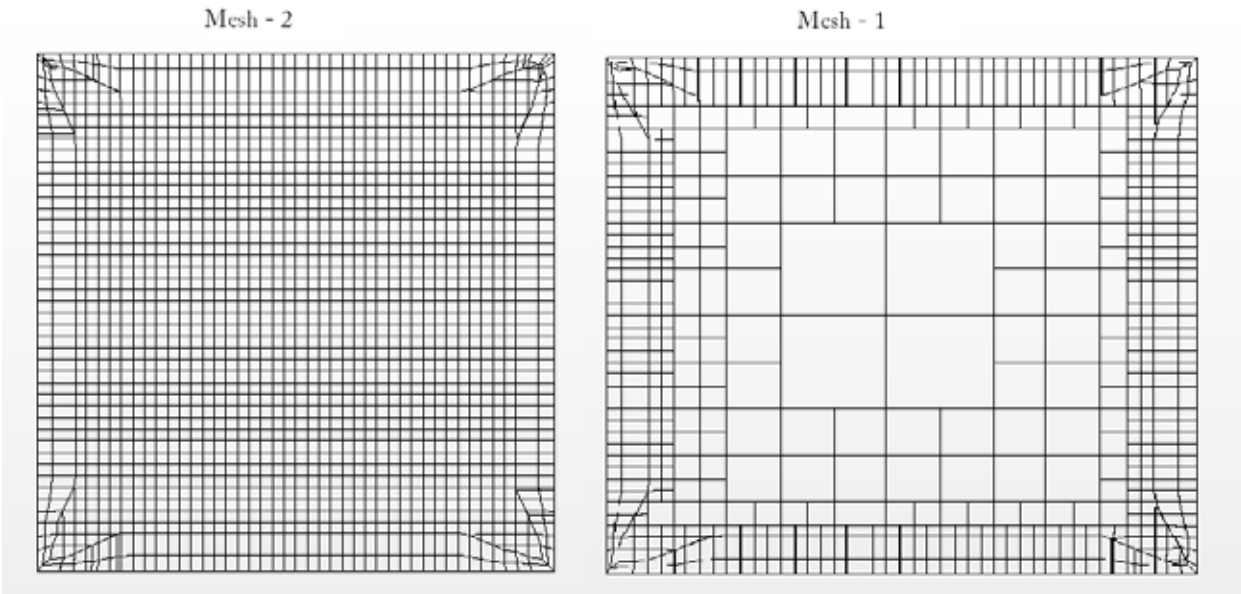

Figure 2.4-3 Radial cross cuts from the two Trim meshes

f) Turbulence model

The default option is used in the code, e.g. 'Realizable k-e Two-Layer and all y+ Wall Treatment'. For more information on this particular model refer to STARCCM+ User guide.

g) Fluid properties

Table 2.4-4 Fluid properties

Reference Temperature (K)	300
Reference Pressure (Pa)	98066.5
Density (kg/m^3)	997.046
Viscosity (Pa-s)	$8.9*10^{-4}$

h) Boundary Conditions

The used boundary conditions are listed in 5.

Table 2.4-5 Boundary conditions

Boundary Group	Location	Boundary Condition
Inlet	Inlet in Figure 2.4-1	Velocity inlet
Outlet	Exit in Figure 2.4-1	Pressure outlet (0 psig)
All others		No-slip wall

RESULTS & CONCLUSIONS

The purpose of this exercise is to test the code (STARCCM) capability (solution accuracy, turbulence) to capture the flow velocity redistribution in the bend caused by the curvature. The flow, being quite symmetric in the straight part redistributes in the bend entrance and assumes a specific velocity profile in the bend middle part (90 Deg).

Two mesh types were used: Polyhedral and Trim. The Trim mesh has several cell types with the majority of them being hexahedral. The polyhedral mesh is composed of polyhedral cells. A moderate cell number was used for the polyhedral mesh, derived based on having around 30 -40 cells in radial direction of the channel, which exceeds slightly the measurement points. No stretching was invoked along the main flow direction. This resulted in 1.86 million cells. The Trim mesh (mesh-1) has lower number of cells because the central channel part is modeled very coarse.

The calculations were run on a linux server in parallel on 4 cores. The residuals from the solutions are shown for the two meshes in Figure 2.5-1.

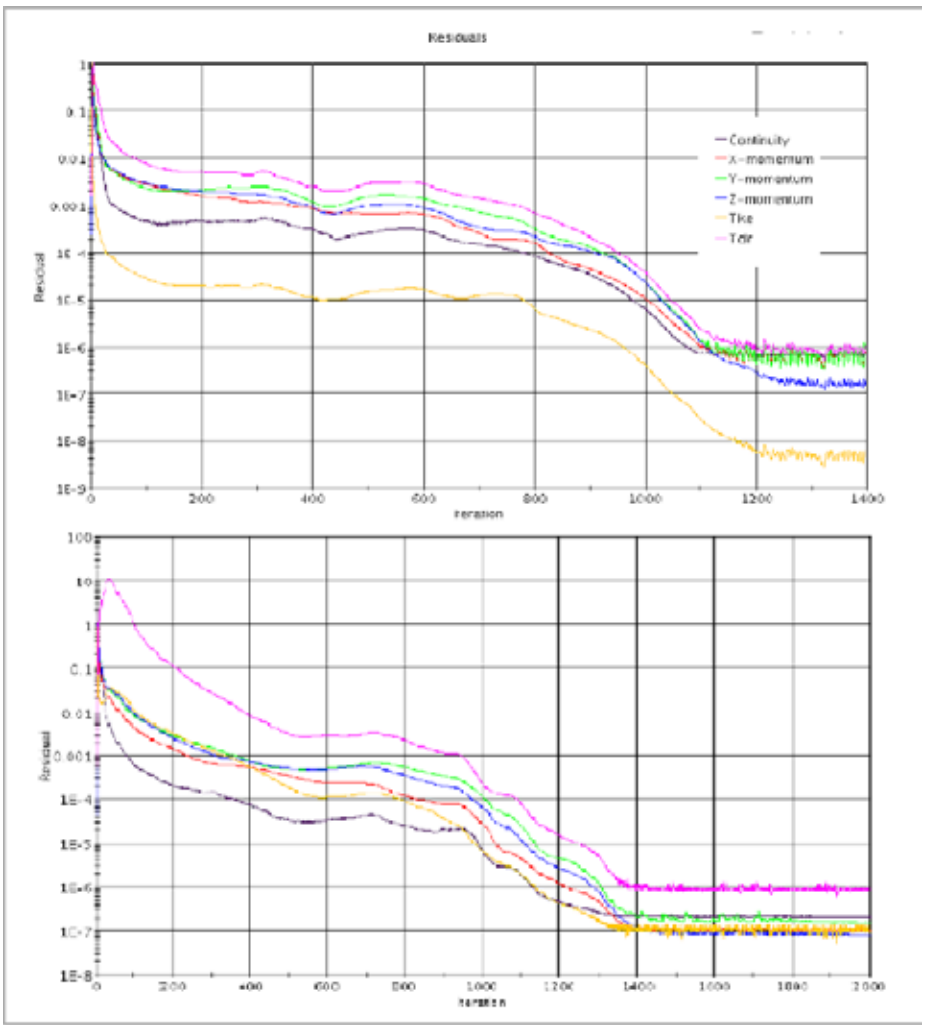

Figure 2.5-1 Poly mesh (top) and Trim mesh (bottom) solution residuals

The two velocity components are compared and discussed here below:

1) Bend entrance X = -1

The velocity magnitude contours are given in Figure 2.5-2 for the two mesh types used. Both meshes give similar results with the Poly mesh giving slightly flatter profile. The plots: Figure 2.6-1 to

Figure 2.6-3 confirm that. We observe one specifics: the test profile shape changes depending on the location, while the computed profile is practically the same with slight difference in the magnitude. The test profile is curved more in the middle (0-location), flat at 0.50, and carved closer to the channel wall. It is not clear what causes these velocity shape differences.

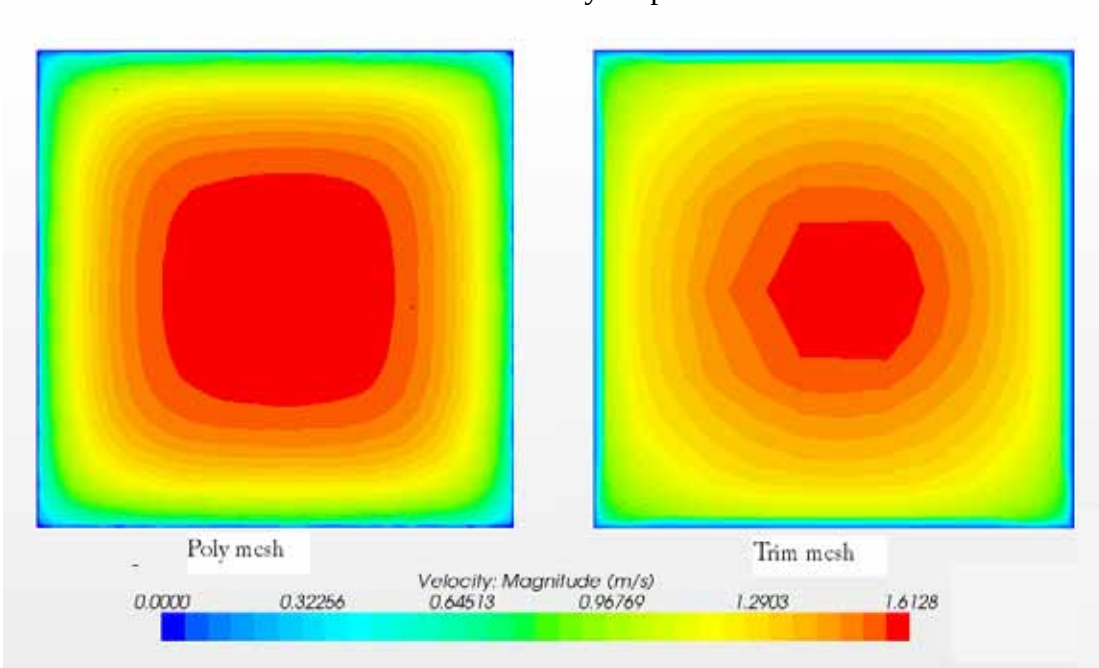

Figure 2.5-2 Theta velocity profiles at X = -1 location

2) Bend mid plane: 90 Deg

The combination of mass flow and channel size in this experiment results in flow redistributing in the entrance part of the bend. To better understand this process, we plotted the Theta velocities at 45 and 90 Deg in Figure 2.5-3. At 45 Deg the midplane profile starts to change, but the velocity is much higher than at 90 Deg same location. Closer to the wall (position 0.75) the situation is opposite, more flow moves next to the wall at 90 Deg than at 45 Deg. The radial velocities are quite the same at the two locations with a noticeable radial drift toward the outer wall only in the central plane of the channel. Based on this we can conclude that the flow redistributes in the bend entrance so that it moves from the center of the channel to the walls, preferentially to the outer wall. The specific feature of this process is a low velocity area formation at 0.3-0.4 radial distance that is well detected in the experiment. Testing the STARCCM ability to capture this phenomenon is the main goal of this exercise.

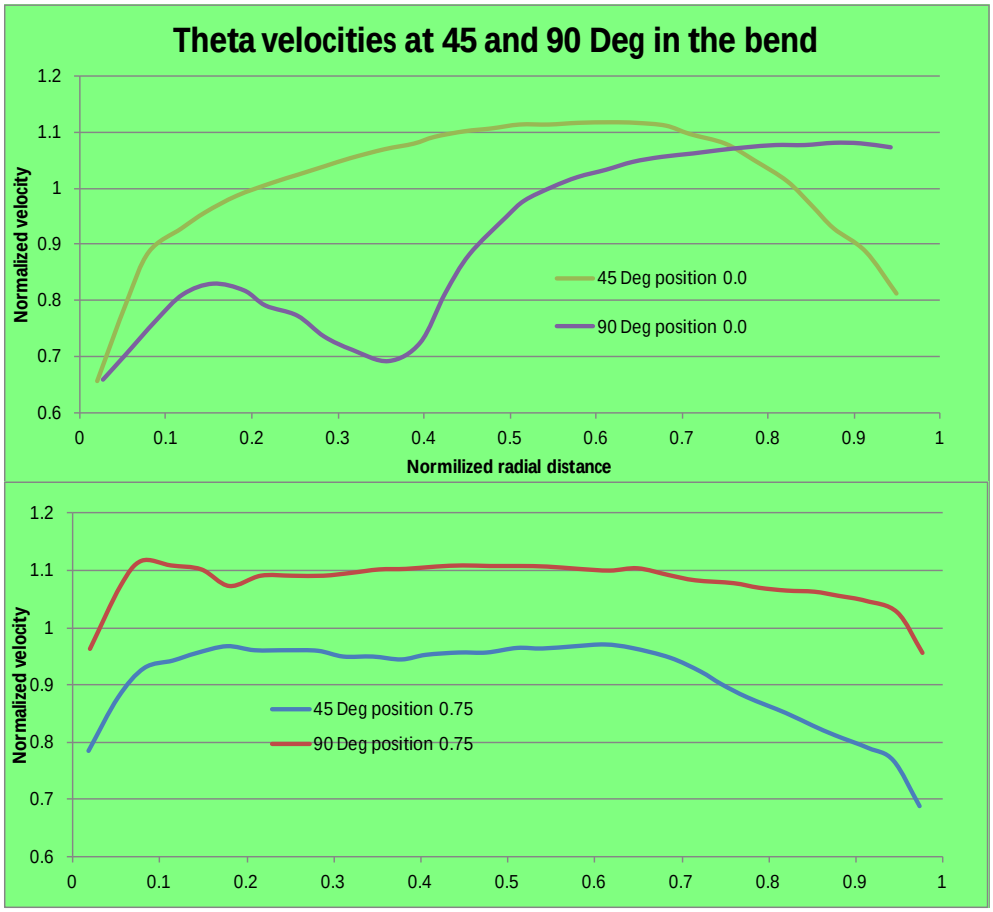

Figure 2.5-3 Theta velocities at 45 and 90 Deg locations in the bend

The velocity contours at 90 Deg location are shown in Figure 2.5-4. It is evident that the Trim mesh does not capture the major flow feature, i.e. the lower velocity area in the center part of the channel. Detail plots of directional velocities are presented in Figure 2.6-4 to Figure 2.6-6, where the same finding is clearly seen. The same turbulence model and other properties and setting have been used in both calculations. The qualitative misinterpretation of the velocity field by the Trim mesh is attributed to the mesh type.

In order to confirm that the solution is converged, another Trim mesh was generated with approximately 3 times more cells and with refined central section (mesh-2). The results from that mesh improved the roughness of the profile at “0” plane, but qualitatively the figure remained the same. No further evaluations of the causes were made.

Bases on this finding it can be concluded that for curved flows the mash type plays a role on the solution. Further investigation of the origin of the problem might be advisable.

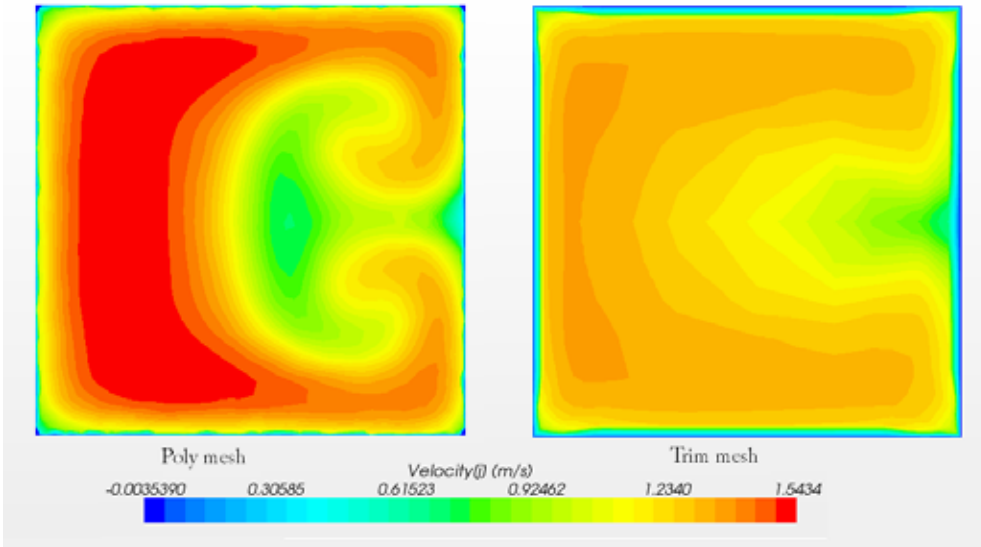

Figure 2.5-4 Theta velocity profiles at 90 Deg location

PLOT DATA

Velocities are plotted for two locations as specified earlier. The STARCCM code uses Cartesian coordinate system and the correspondence to the test data for the reported velocities is as follows:

- X = -1 location: Theta velocity equals –X velocity in STARCCM; Radial velocity equals Y velocity in STARCCM
- 90 deg location: Theta velocity equals -Y velocity in STARCCM; Radial velocity equals X velocity in STARCCM

The X = -1 location velocities are plotted in Figure 2.6-1 to Figure 2.6-3, and 90 Deg velocities are plotted in Figure 2.6-4 to Figure 2.6-6.

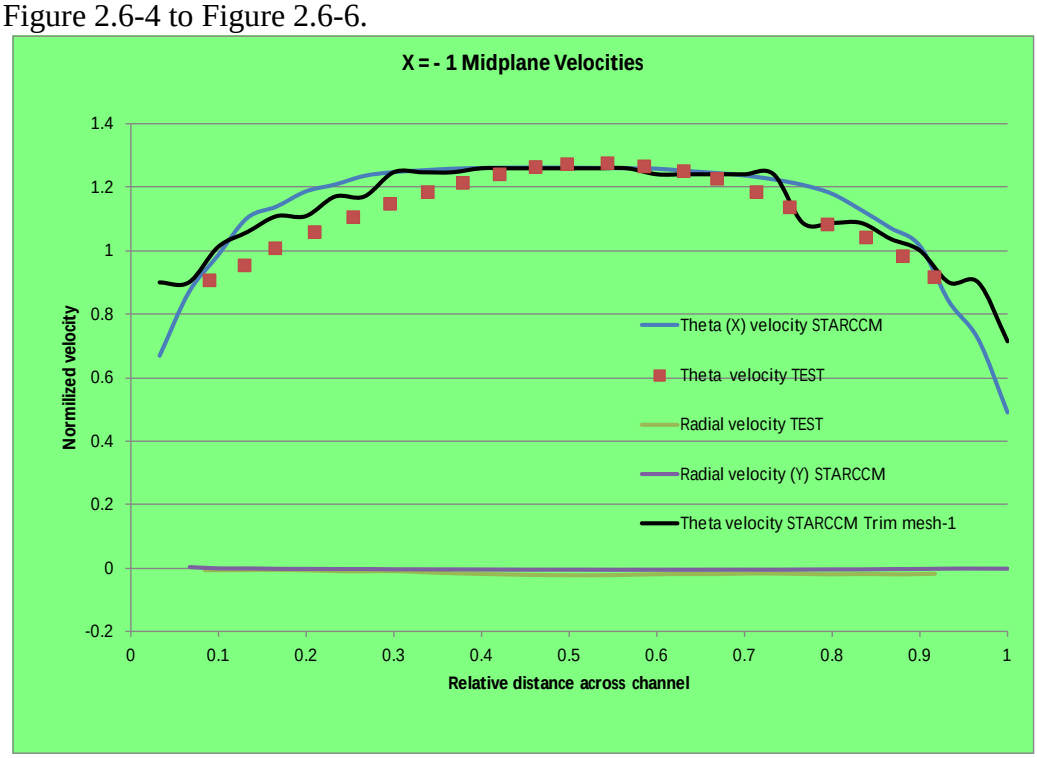

Figure 2.6-1 Plane 0 Theta velocities at X = -1 location

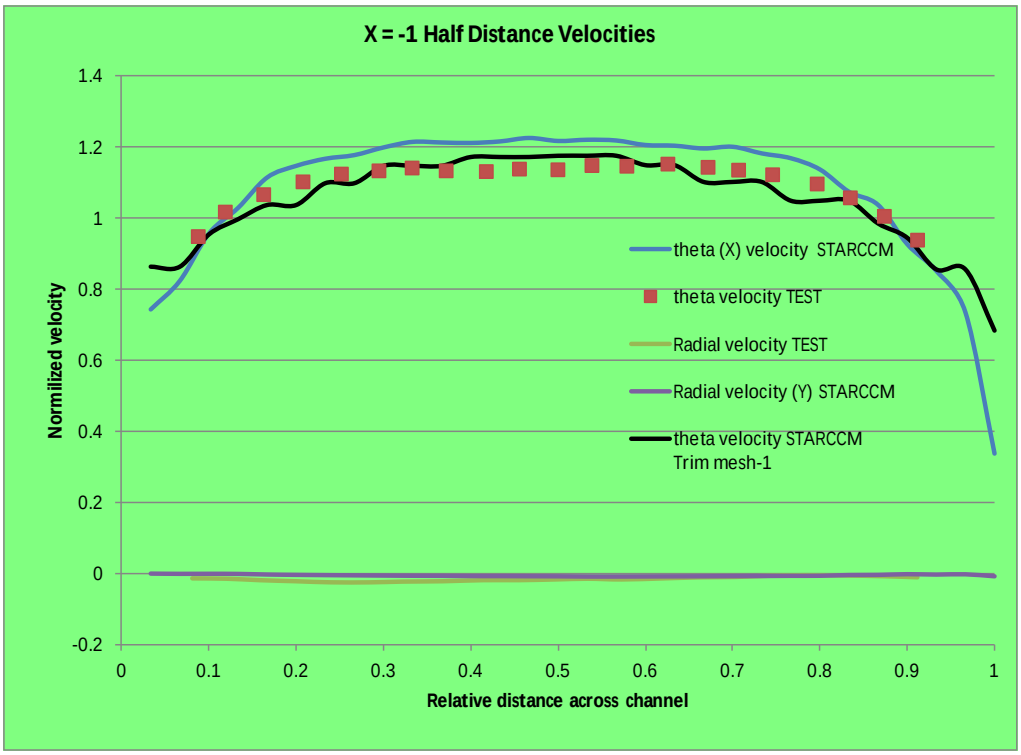

Figure 2.6-2 Plane 0.5 Theta velocities at X = -1 location

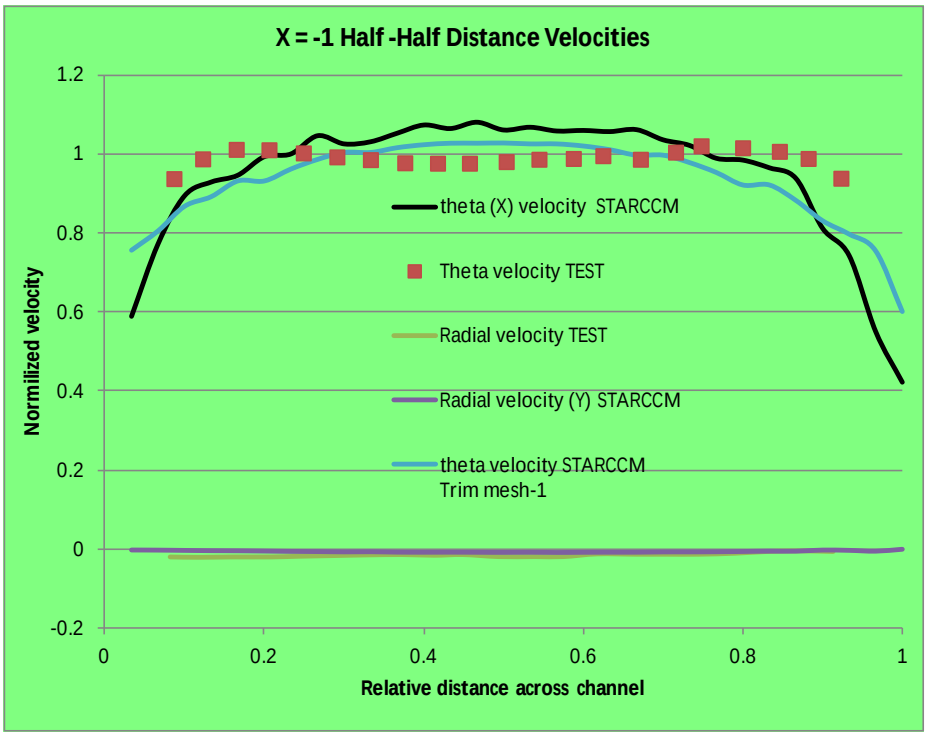

Figure 2.6-3 Plane 0.75 Theta velocities at X = -1 location

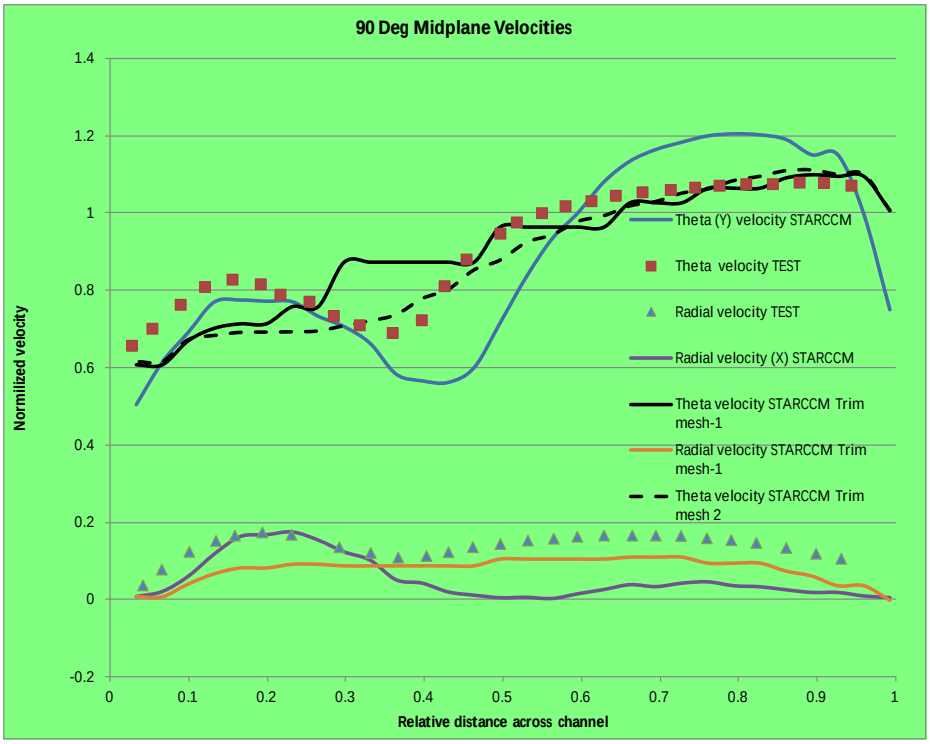

Figure 2.6-4 Plane 0 Radial velocities at 90 Deg location

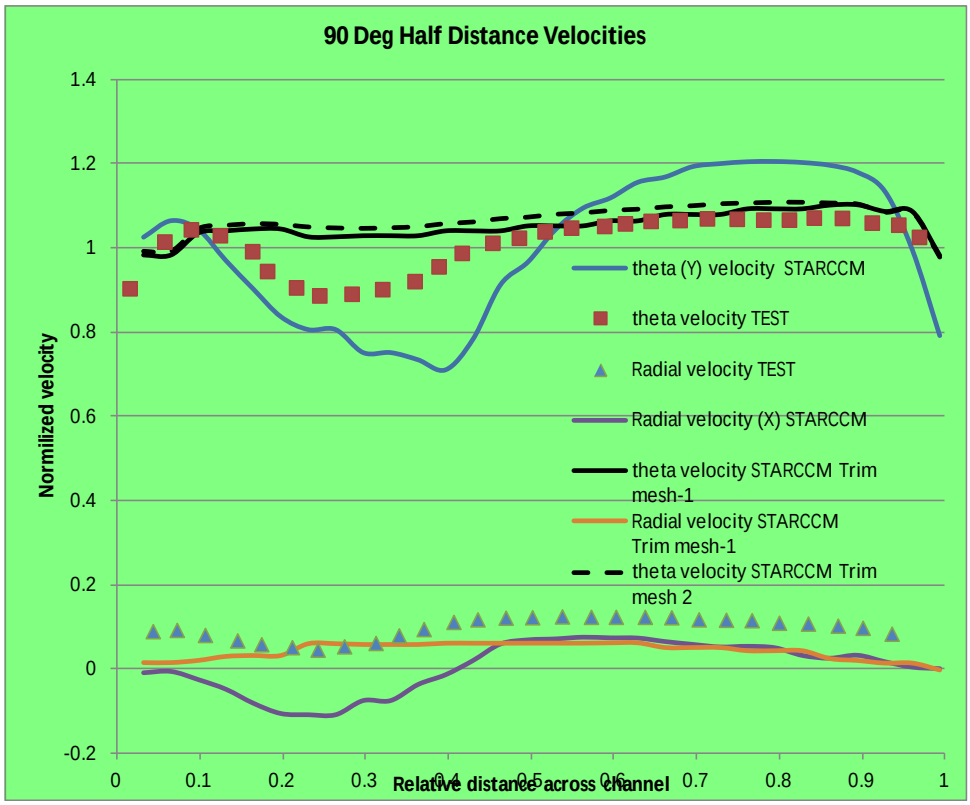

Figure 2.6-5 Plane 0.50 Radial velocities at 90 Deg location

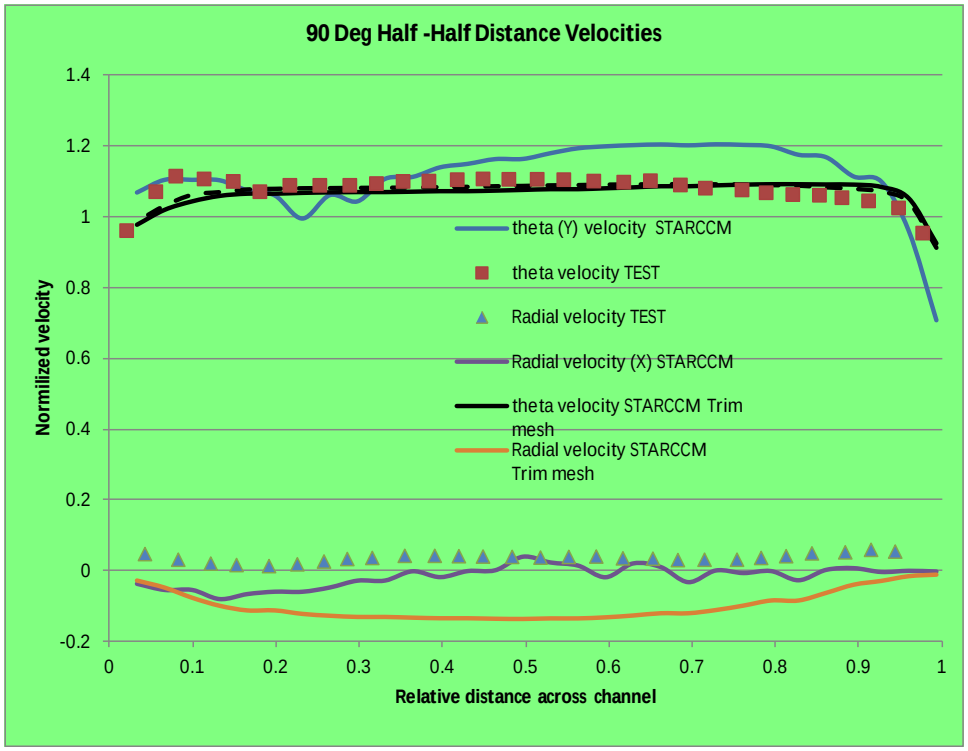

Figure 2.6-6 Plane 0.75 Radial velocities at 90 Deg location

REFERENCES

2.1. "Turbulent Flow in a Strongly Curved U-Bend and Downstream Tangent of Square Cross-Sections", Physico-Chemical Hydrodynamics, vol 4, no 3, pp. 243-269, 1983.

2.2. J.A.C. Humphrey, S.M. Chang, and A. Modavi, "Developing turbulent flow in a 180 degree bend and downstream tangent of square crosssections", Report No. LBL-14844, Lawrence Berkeley Laboratory, University of California, Berkeley (1982).

Validation Case 3: Flow in the 5 × 5 Rod Bundle with Spacer-Grids

OBJECTIVES

The objective of this activity is to benchmark the Computational Fluid Dynamics (CFD) analysis with experimental data for the flow in a 5 × 5 rod bundle with spacer-grids.

Using current state of the art experimental techniques, the experimental data was acquired at the Advanced Optical Multiphase Flow Research Laboratory (AOMRL) of Texas A&M University. The test rig includes a 5 × 5 rod bundle with four spacer grids and two vaneless support grids.

For the CFD model, a 3D SolidWorks CAD model of a 5 × 5 rod bundle with one spacer grid and one vaneless support grid was constructed based on drawings, which represents the geometry of the middle section of the test rig. The major dimensions of the CAD model are kept the same as those of the test rig.

PROBLEM DESCRIPTION

The flow housing is a rectangular acrylic channel with a square cross section of 66.675 mm side length and 1828.8 mm long as shown in Figure 3.2-1. Water is used as a working fluid.

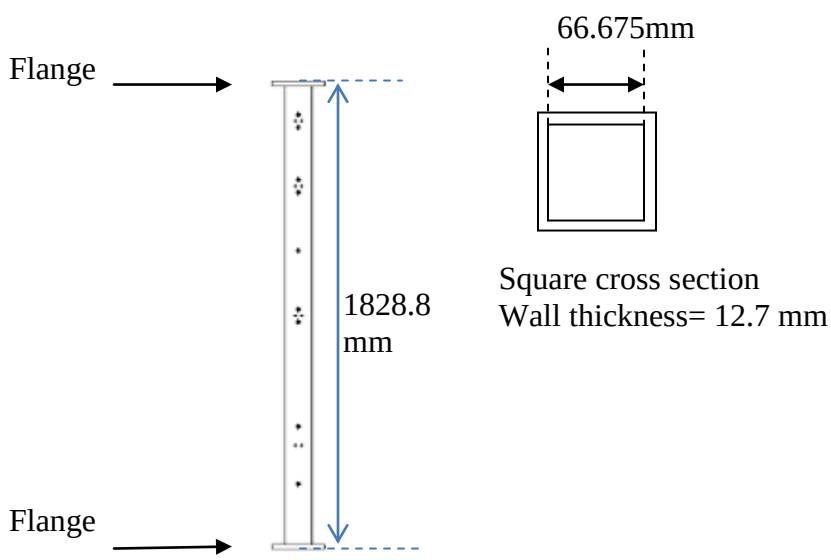

Figure 3.2-1: Acrylic flow housing

The tested rod bundle consists of 25 plastic rods with an ID of 9.5 mm placed in a 5 × 5 configuration. The rods are kept in place using four spacer-grids with Westinghouse V5H mixing vanes and two Westinghouse simple support grids. The grids with mixing vanes are positioned inside the flow housing using two set-screws (#10-24) on each face of the grid for a total of 8 screws per grid. The simple support grids are not attached to the flow housing. The location of the six spacer-grids along the flow housing and its corresponding name are shown in Figure 3.2-2. The distances between spacer-grids as shown in Figure 3.2-2 are measured from bottom to bottom of the

spacer. The distance between the edge of the grid and the wall of the flow housing is 1.2 mm for the four faces.

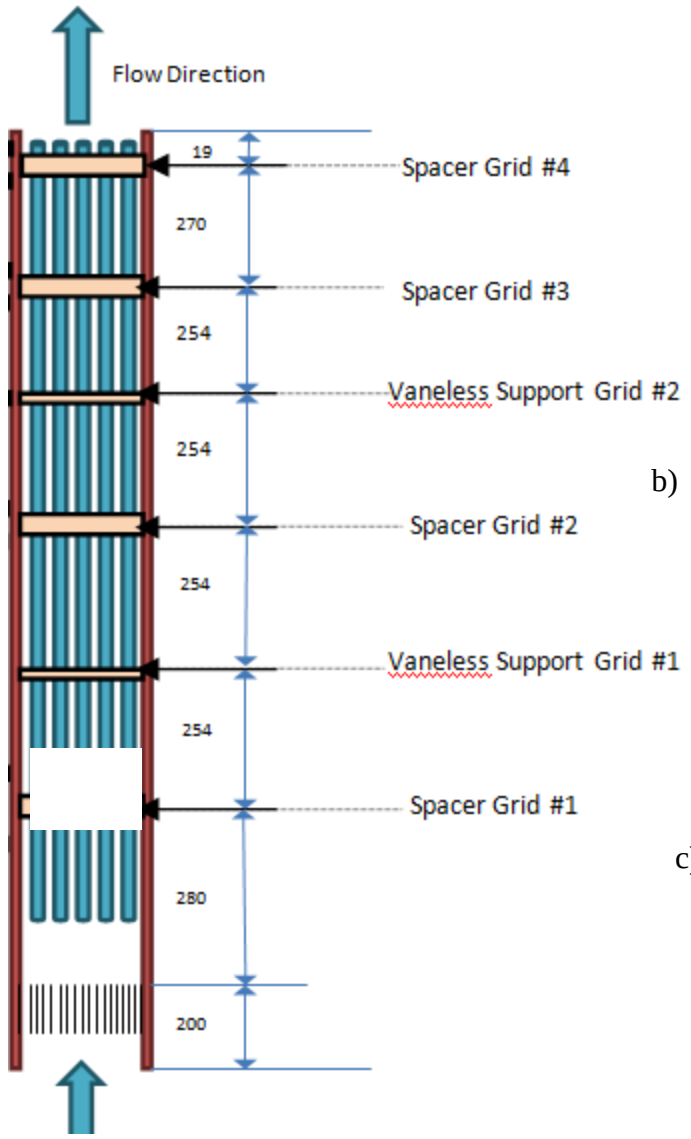

a) Front view

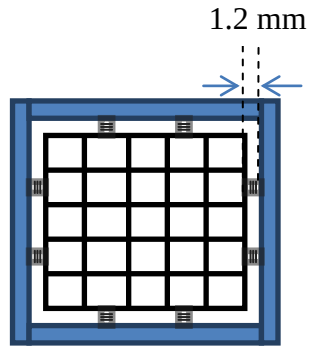

b) Top view of the rod bundle inside flow housing

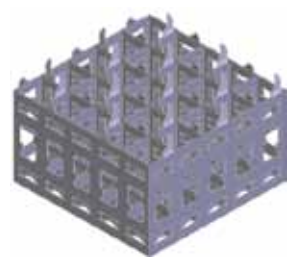

c) Details of spacer-grid with mixing vanes

Figure 3.2-2: 5 × 5 Rod bundle inside flow housing

The test rods used in the test bundle were fabricated using a fluorinated ethylene-propylene (FEP) plastic with dimensions of 9.5 OD × 9 ID x 1270 mm long with a ± 0.0762 mm tolerance in all dimensions. This tube material was chosen to match the refractive index of water. Therefore, these tubes are optically transparent when immersed in water during the testing. For reinforcement away from the measurement region, thicker acrylic tubes were inserted from the top and bottom inside the FEP tubes to maintain rod rigidity during testing. This ensures that the rods are maintaining the appropriate rod pitch in the ungridded regions and restrict rod vibration under flow conditions.
The general characteristics of the tested bundle are shown in Table 3.2-1.

Table 3.2-1: General parameters of the tested bundle

	Pitch (P) (mm)	**Average rod outside diameter (mm)**	**Hydraulic diameter (Dh) of subchannel between 4 rods**	**Distance between spacers (mm)**
Grid with vanes	12.6	9.5	11.78	508

Only the flow field is simulated in the simulation. Fluid domain was built in 3D CAD package SolidWorks. The simulation section includes one spacer grid and one vaneless support grid as shown in Figure 3.2-3.

The distance from inlet to the bottom surface of space grid is 107.95 mm which is about the half of the fluid height between support grid #1 and spacer grid #2 (See Figure 3.2-2). The distance from the top surface of support grid to outlet is 54.61 mm, which is about half of the fluid height between support grid #2 and spacer grid #3 (See Figure 3.2-2). Therefore, the simulated section is the middle section of the test rig, i.e. to simulated flow between support grid #1 and spacer grid #3.

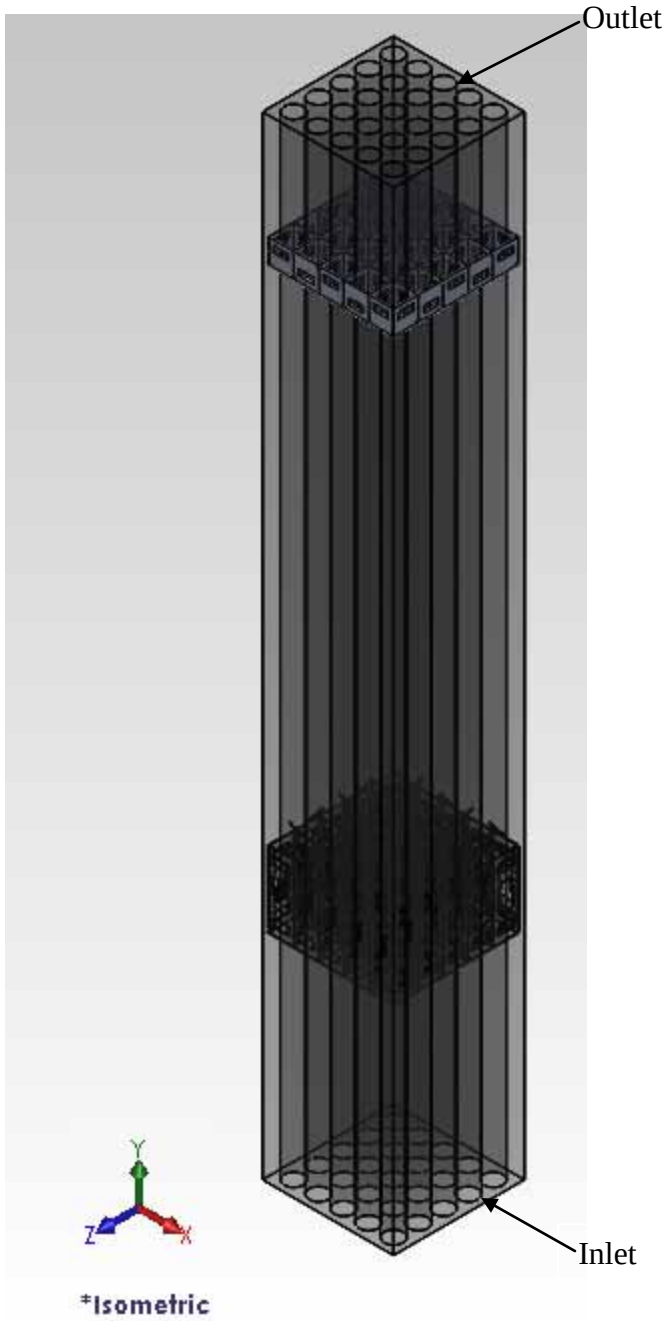

Figure 3.2-3: Fluid domain

KEY PARAMETER COMPARISONS: AXIAL AND LATERAL VELOCITY

The contour of axial (V) and lateral (U) velocity component was compared between CFD and simulation and experimental data on 3 planes (i.e. plane 5, 6 and 7 as shown in Figure 3.3-1 and Figure 3.3-2). In the x and z direction, these 3 planes cover all fluid zone and in the y direction, they cover elevation from 0 mm (measured from the grid welding nugget) to 55 mm downstream.

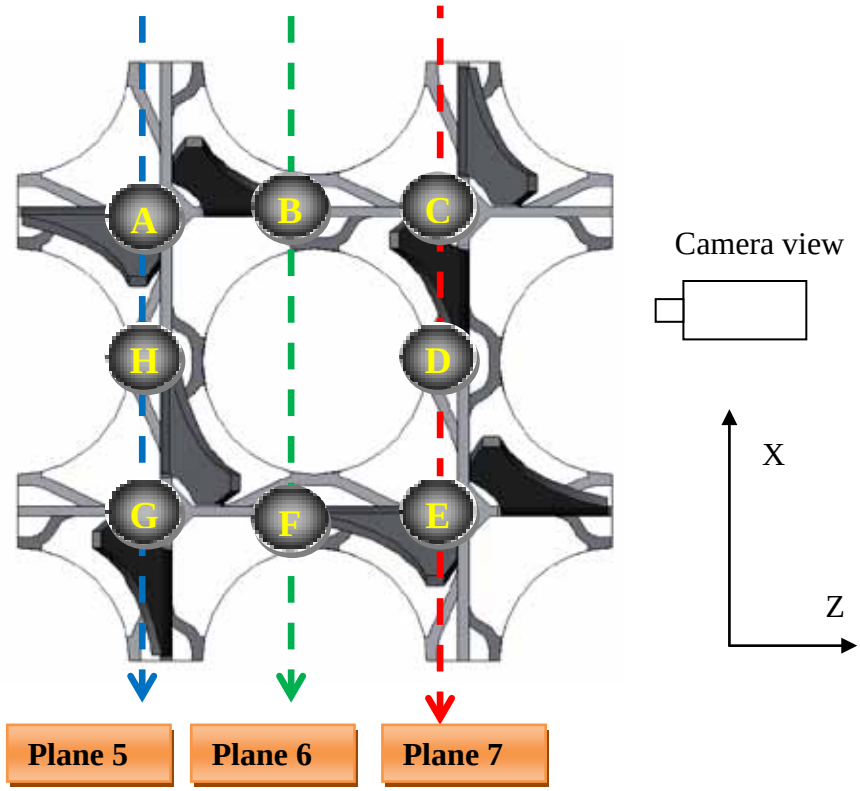

Figure 3.3-1: The data sample locations

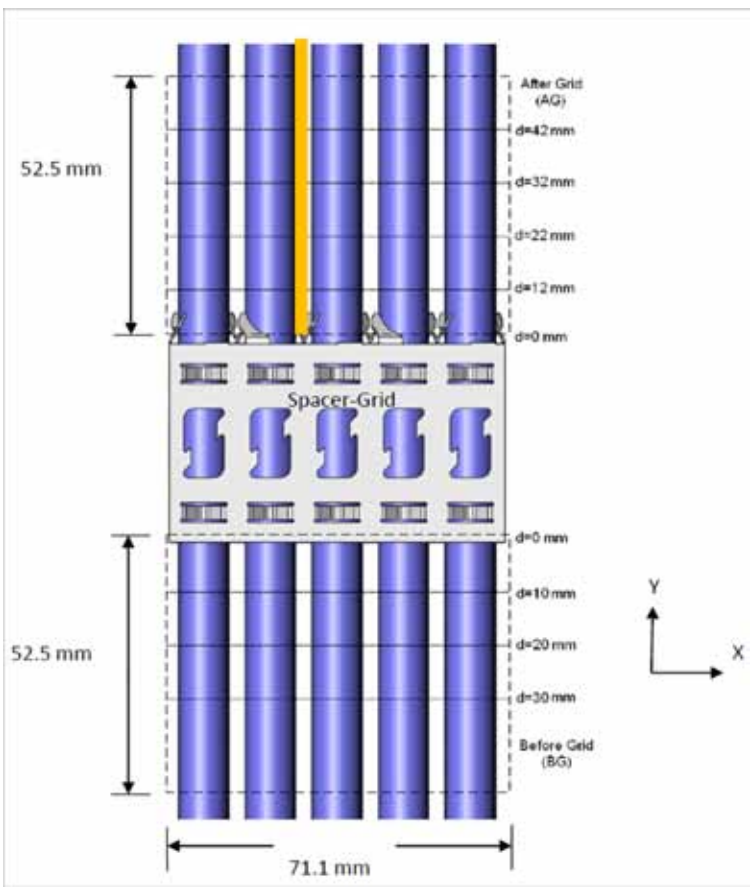

Figure 3.3-2: Y elevation for planes 5, 6 and 7 (yellow line)

CFD MODEL INFORMATION

a) Software and Version:

STARCCM+ computer code is used for the simulation, version: 6.04.014, running on Westinghouse server "fever".

b) Physical Models:

The following physical models were used in the simulation:

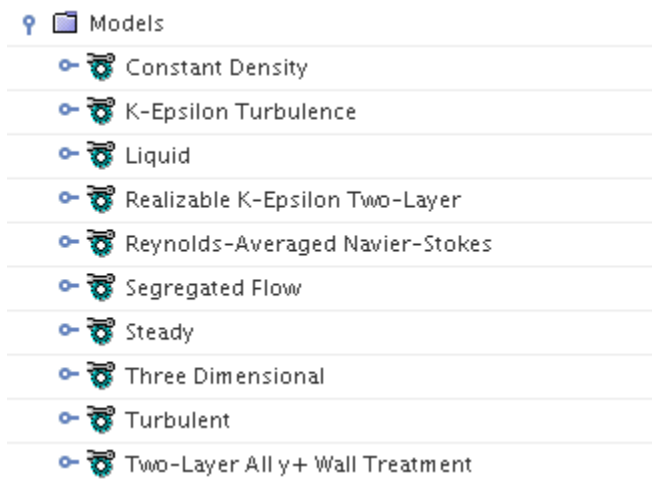

c) Solver:

Segregated steady flow. AMG V-cycle for pressure and turbulence and Flex cycle for velocity. Relaxation: Gauss-Seidel, acceleration for pressure – Conjugate Gradient.

d) Descretization Schemes used in the model:

Second order convection for all properties.

e) Domain:

See Figure 3.2-3.

f) Mesh information, cell type, cell count, meshing parameters:

The Trimmer mesher was used with prism layer specified at wall boundaries to capture boundary layer. The total mesh has 181126173 cells. Figure 3.4-1 and Figure 3.4-2 show the mesh at outlet boundary. As can be seen from these figures, inflation layers are generated around fuel rod wall. Figure 3.4-3 shows the mesh at spacer grid walls and Figure 3.4-4 shows mesh at support grid walls.

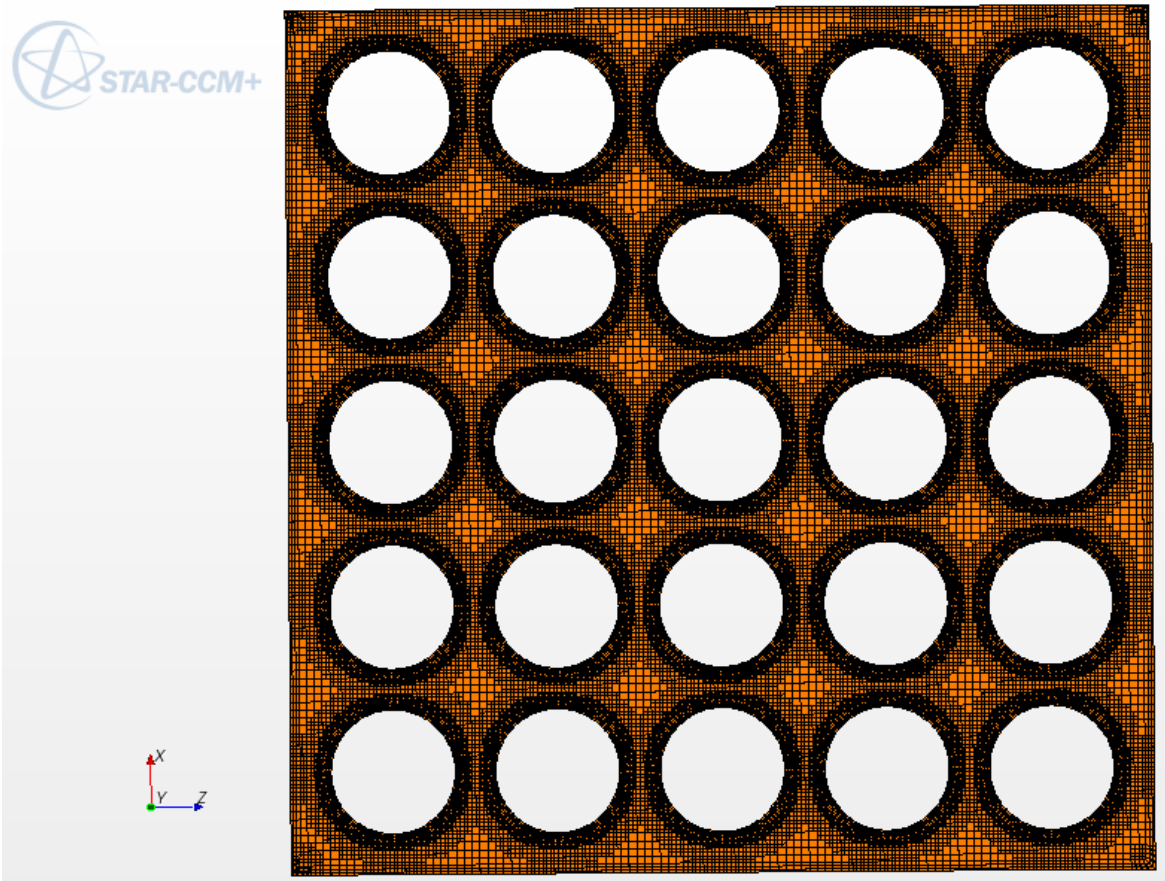

Figure 3.4-1: Mesh at outlet boundary

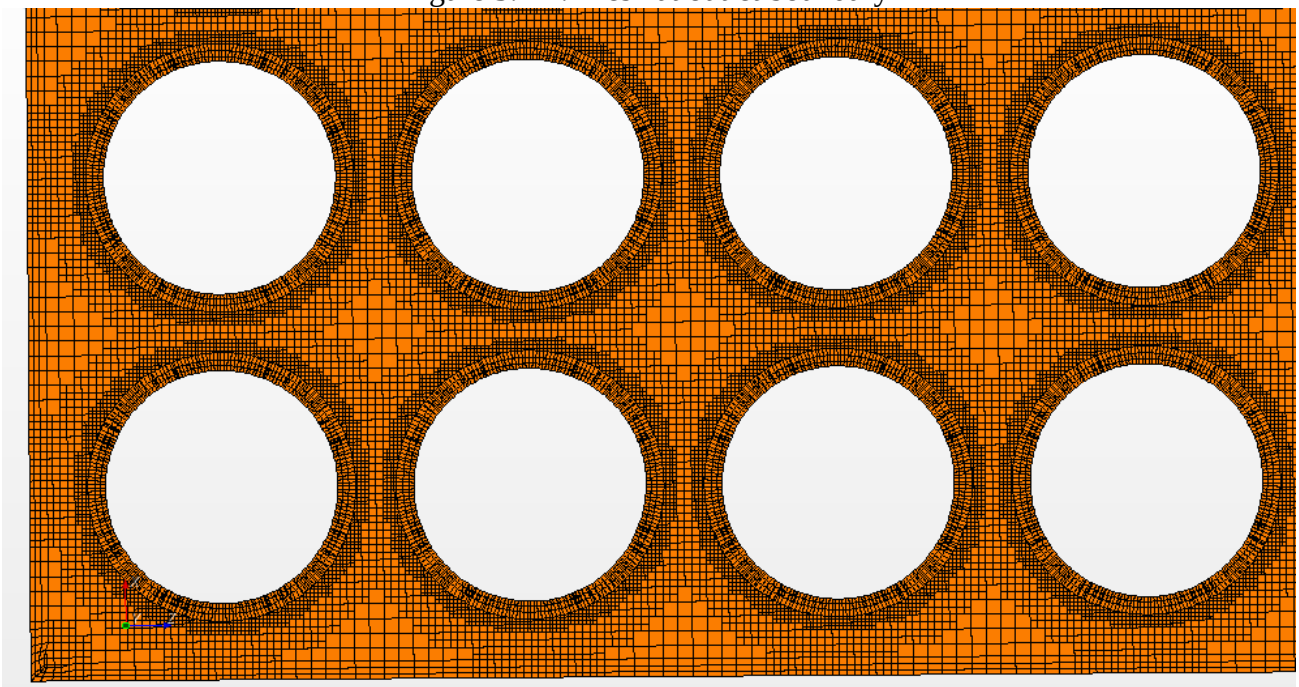

Figure 3.4-2: Mesh at outlet boundary (zoomed in view)

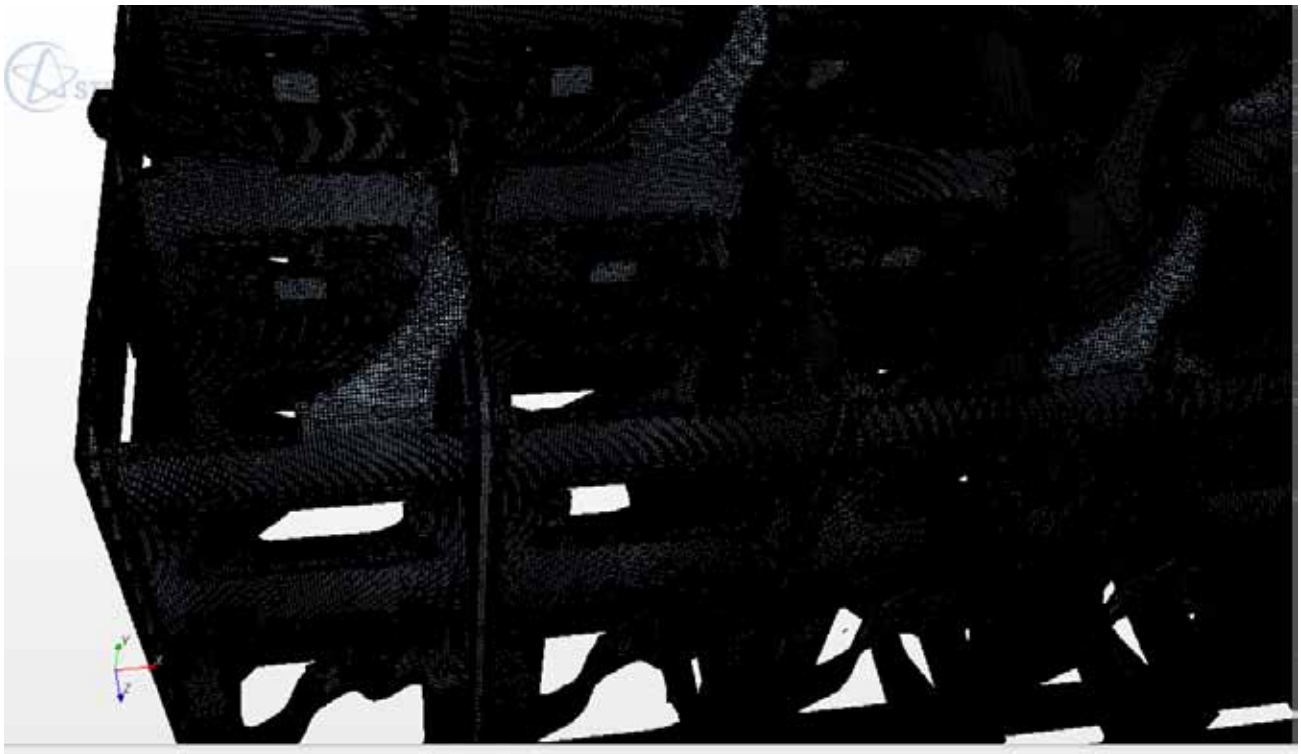

Figure 3.4-3: Mesh at spacer grid walls

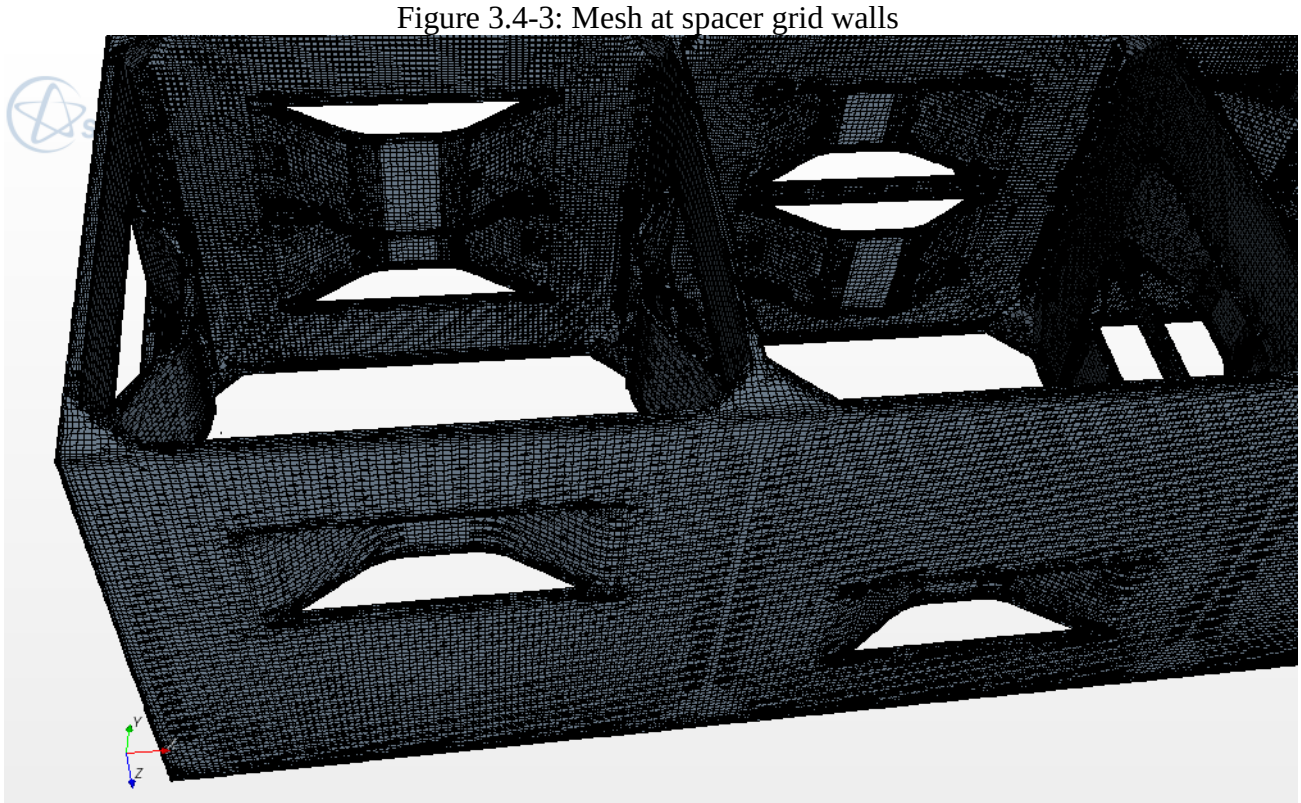

Figure 3.4-4: Mesh at support grid walls

A trim mesh with 38.7 M hexahedral cells were created. The mesh size and configuration follow Westinghouse internal best practice on meshing for fuel assembly.

g) Turbulence model:

The default turbulence option i.e. 'Realizable k-e Two-Layer and all y+ Wall Treatment' is used.

h) Fluid properties:

Fluid is water at 1 atm and 24˚C. Water density is 997.561 kg/m^3.

i) Boundary Conditions:

Inlet: Velocity inlet of 2.48 m/s.
Outlet: Pressure outlet of zero relative pressure.
All other boundaries are no-slip wall boundary.

RESULTS & CONCLUSIONS

The calculations were run on Westinghouse server "fever". The run was stopped manually when small solutions residuals are achieved and the solution is judged to be converged.

The comparison between CFD simulation and experimental data for the contour of axial (V) and lateral (U) velocity component on the 3 planes (plane 5, 6 and 7) are shown in Figures 3.5-1 through 3.5-6. It can been seen from figures that for the steady state result, the CFD result is in relative good agreement with experiment data in terms of trend and absolute value. The agreement between CFD and experiment was also demonstrated by the resemblance between CFD result and experiment data for the contour plots of axial and lateral velocity component as shown in Figures 3.5-1 through 3.5-6.

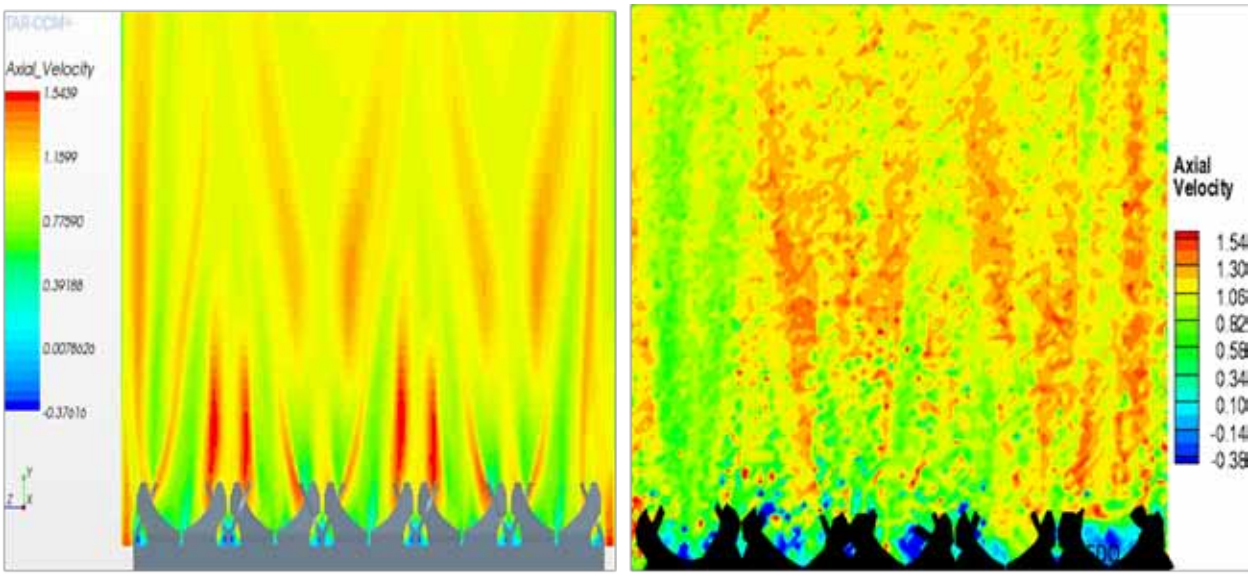

Axial velocity CFD. Plane 5 Re=28,000 Axial velocity Measured. Plane 5 Re=28,000

Figure 3.5-1: Comparison of axial velocity at plane 5

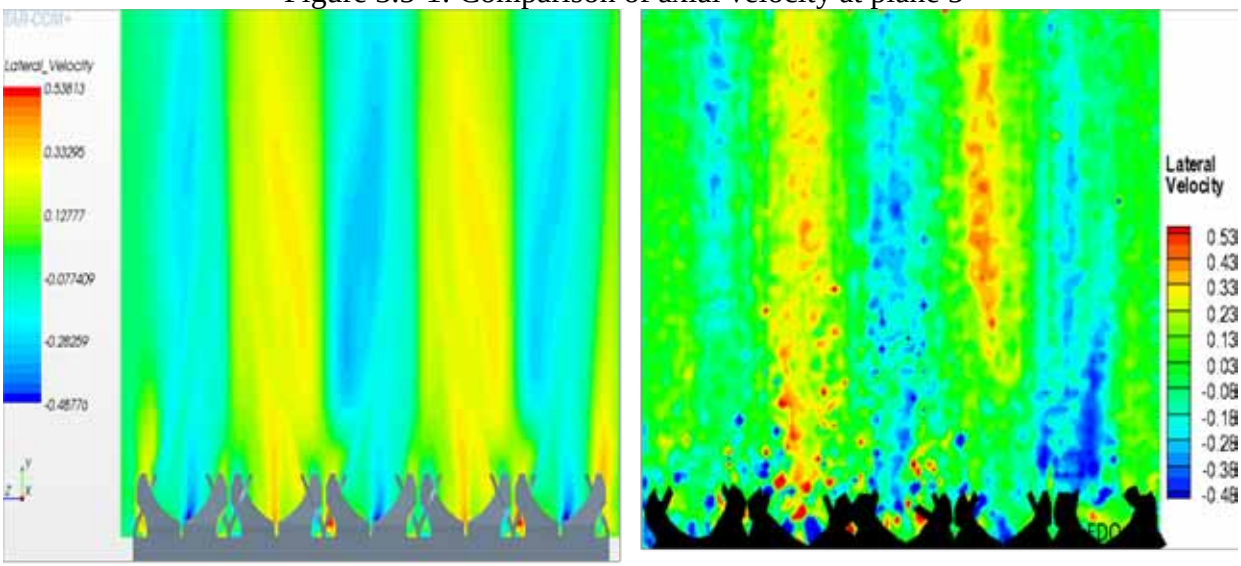

Lateral velocity CFD. Plane 5 Re=28,000 Lateral velocity Measured. Plane 5 Re=28,000

Figure 3.5-2: Comparison of lateral velocity at plane 5

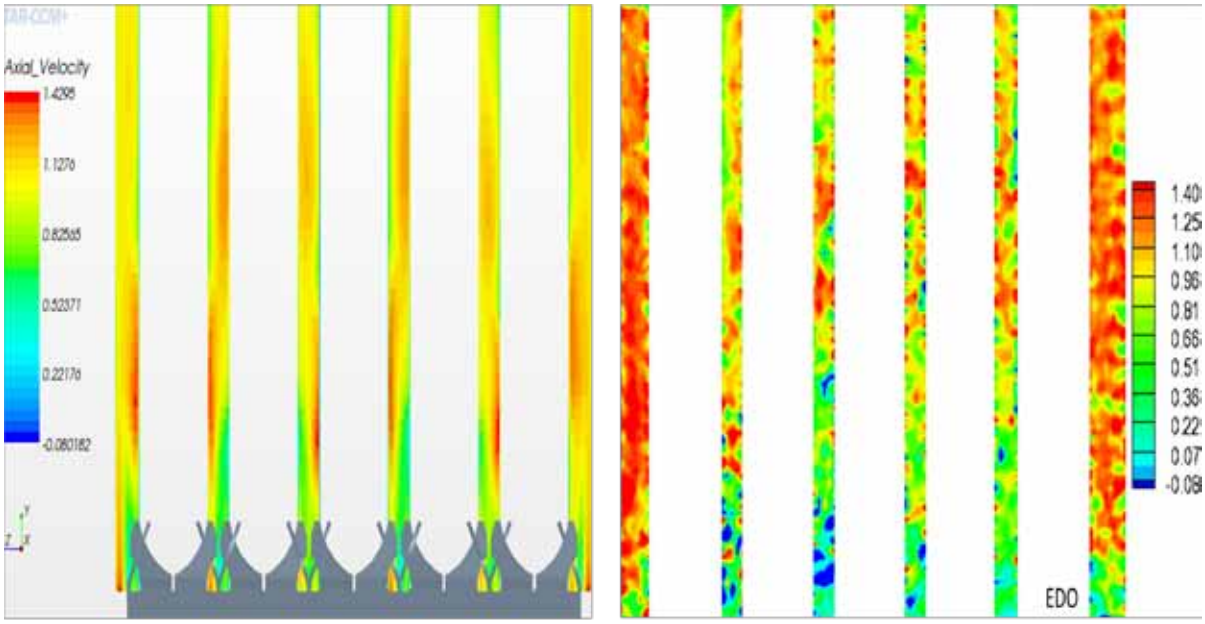

Axial velocity CFD. Plane 6 Re=28,000 Axial velocity Measured. Plane 6 Re=28,000

Figure 3.5-3: Comparison of axial velocity at plane 6

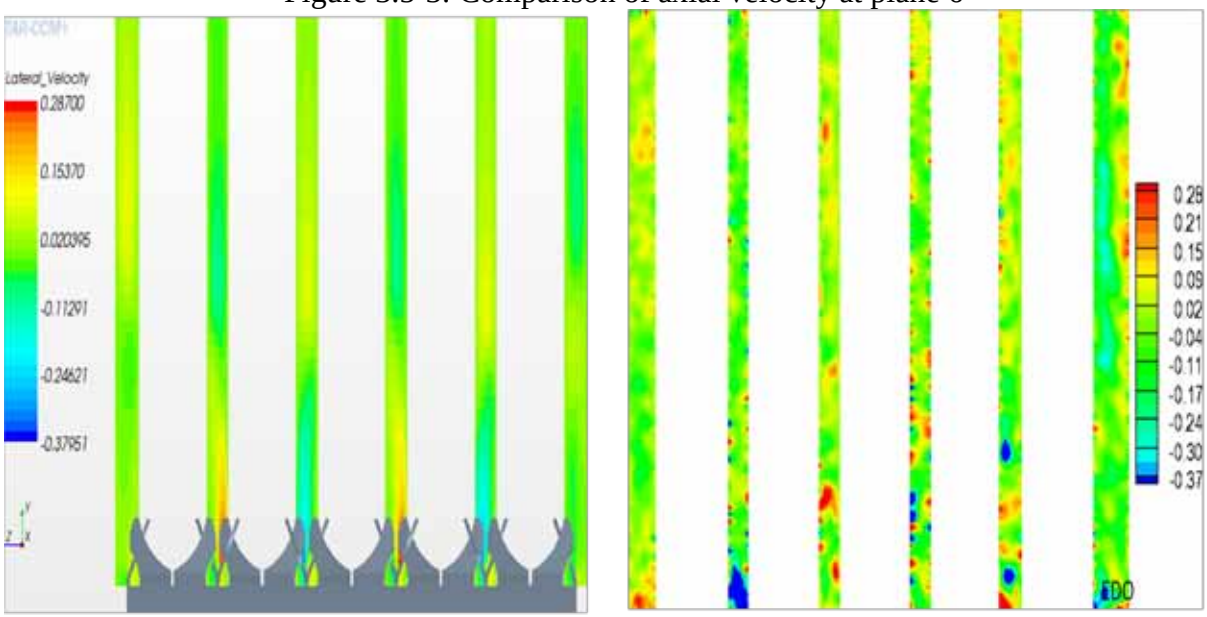

Lateral velocity CFD. Plane 6 Re=28,000 Lateral velocity Measured. Plane 6 Re=28,000

Figure 3.5-4: Comparison of lateral velocity at plane 6

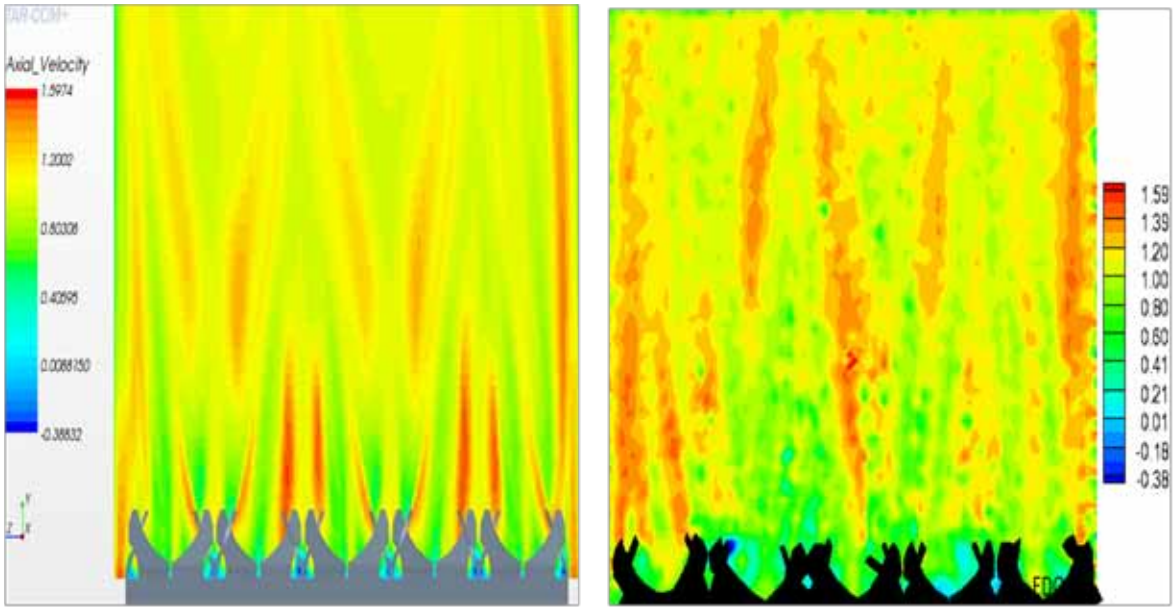

Axial velocity CFD. Plane 7 Re=28,000 Axial velocity Measured. Plane 7 Re=28,000

Figure 3.5-5: Comparison of axial velocity at plane 7

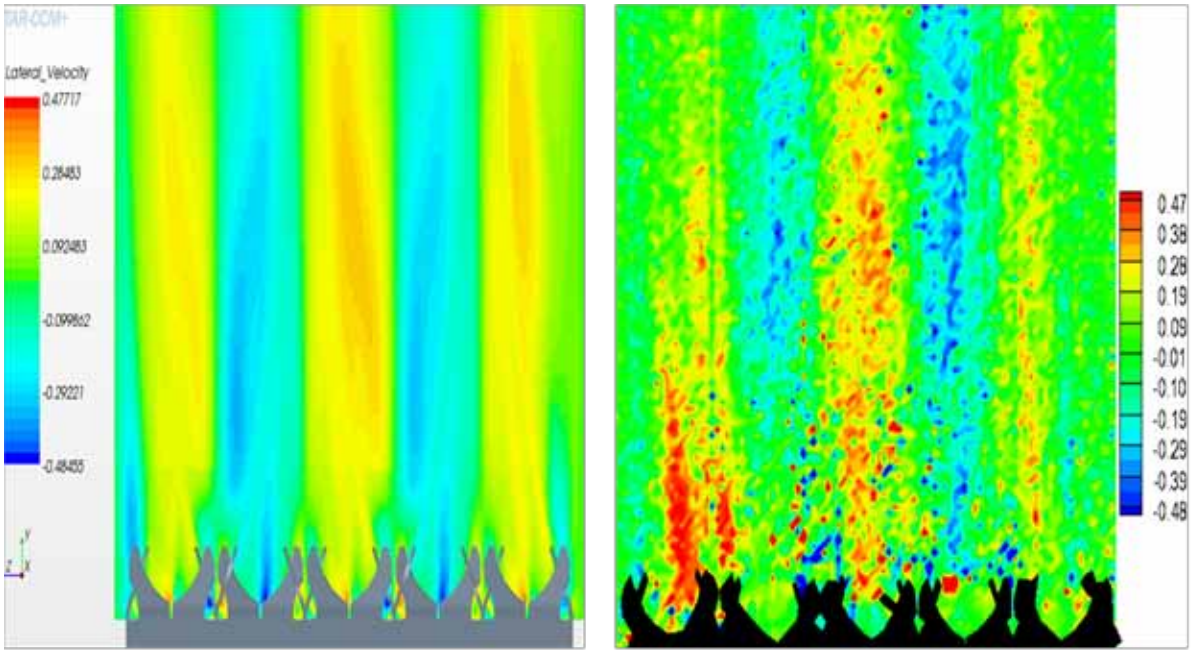

Lateral velocity CFD. Plane 7 Re=28,000 Lateral velocity Measured. Plane 7 Re=28,000

Figure 3.5-6: Comparison of lateral velocity at plane 7

FUTURE WORK

It is suggested to use Large Eddy Simulation (LES) model to simulation turbulence for the future and then compare LES result with transient experiment data.

Validation Case 4: Flow Passing Heated Rod Bundle

Abstract

A preliminary analysis was performed with Star-CCM+ for Test Case 4 of the CASL suite of V&V problems, shown here.

Relevance: flow past heated rod bundles is relevant to PWR channel flow past fuel rods.
Objectives: To validate modeling of anisotropic turbulent flow with conjugate heat transfer in rod bundle geometries.
Descriptions: air flows into a horizontal, 37-rod bundle in triangular array with prescribed heat flux.
Requested calculations and metrics: wall temperature distribution.
Validation database: "Measurements of turbulent velocity and temperature in axial flow through a heated rod bundle", L. Meyer, Nuclear Engineering and Design, 146, pp. 71-82, 1994.
Reference: "Anisotropic Turbulence Modeling for Accurate Rod Bundle Simulations", E. Baglietto, ICONE14-89646, July 2006.

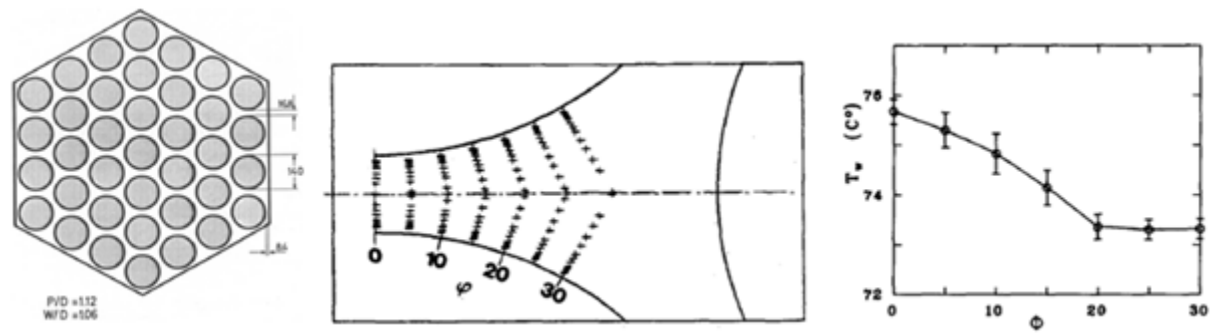

(a) Rod Bundle Distribution (b) Meassuring Positions ina central channel (c) Wall Temperature

Figure 4.1 Validation Case 4: Flow Passing Heated Rod Bundle

The model was built in Solid Works and extruded one centimeter in the flow direction. A 22.7 m/s inlet velocity condition was imposed with a pressure outlet boundary for the air as a fluid. Material properties were those used by Baglietto [4.1]. The inlet room temperature of 294 K was used at the inlet and outlet (in case of flow reversal) and as the initial condition for the model. The Monel layer on the outside of the epoxy rod was fifty micrometers in thickness. A special imprint/merge option in Star-CCM+ was used to mesh the thin layer of Monel. Two different meshes were used for a heat source in the Monel metal and both gave good results compared to the data, shown here for the temperature around the center rod.

Relevance to CASL:

Flow past heated rod bundles is clearly relevant to PWR channel flow past fuel rods.

Objectives:

This test case tests the ability to model anisotropic, single-phase, turbulent flow with conjugate heat transfer in rod bundle geometries.

Description:

A rod bundle of 37 parallel rods with outer diameter D = 140 mm arranged in triangular array in a hexagonal symmetric channel is illustrated in Figure 4.1. The channel is oriented horizontally. The total length L of the working section is L = 11.50 m with an unheated entrance length L_{iso} = 4.60 m and a heated length of L_{heat} = 6.90 m. The pitch to diameter ratio of the rods is P/D = 1.12, corresponding to a length to hydraulic diameter ratio for the heated section of L_{heat}/D_h = 128. The rods are made of epoxy reinforced with fiberglass and sheathed with a 50 µm foil of Monel metal, which serves as a resistance heating element, as illustrated in Figure 4.2. The channel walls are constructed of aluminum covered on the outside with thick insulation to minimize heat loss. The entire bundle is constructed from five sections, each 2.30 m long. The rod gap spacers are made of 4mm thick and 15 mm wide (in axial direction) steel with rounded edges. Meyer reported the deviations from the nominal bundle geometry to be less than 0.2 mm.

Air at atmospheric pressure (1.01325 x 10^5 Pa) and room temperature (assumed 70 ^{o} Fahrenheit) flows into the entrance. Prior to this, it passes through an entrance section of length 5 m with honeycomb grid and a number of fine grid screens. Measurements were performed at a position 20 mm upstream of the outlet in a central channel next to the central rod. Data for the heated experiment were: Reynolds×10 number Re = 6.65 x 10^4 with bulk velocity in the central channel u_b = 22.7 m/s and a bulk temperature T_b = 52.8□C. Material properties are summarized in Table 4.1.

Calculation by Baglietto:

The calculation performed by Baglietto in the ICONE14 report [4.1] **was not performed with Star-CCM+** but with STAR-CD. Star-CCM+ does not have a hexahedral meshing capability but STAR-CD does. This problem was performed by Baglietto with Star-CCM+ but was never published [4.2]. This is the first time that the problem has been performed external to CD-ADAPCO with Star-CCM+.

In the article by Meyer, the heat flux around the perimeter of the rods is assumed to be uniform with a value of 1.37 W/m^2 (estimated error of 1.5%), but this assumption is claimed to be inaccurate by Baglietto in the ICONE14 report.

Baglietto's models are shown in Figure 4.3. The upper model consisted of a heat flux on the inside of the fluid and the lower model consisted of a heat source in the Monel metal. The results for each are shown in Figure 4.4 compared to the data. Baglietto's comparisons to this data using the improved turbulence model and a standard k-ε model are given in Figure 4.4. Meyer measured wall temperatures with an infrared pyrometer with uncertainty of 0.5C.

Baglietto obtained the correct wall temperature profile only by solving the conjugate heat transfer problem and utilizing his anisotropic eddy viscosity model. This calculation assumed a uniform volumetric heat source in the Model foil consistent with Meyer's reported flux of q = 1.37 W/m^2. Note that due to geometrical discretization of the cylindrical geometry, a heat source correction may be needed to insure that the total power generated is correct.

Requested calculations and metrics:

Wall temperature is requested as a function of angle for comparison to the experiment. Similarly, comparison of the calculation for heat flux to compare to Baglietto's STAR-CD calculation. In addition, non-dimensional velocity and temperature values in the channel are requested for comparison to the data in Figure 7 of the reference. Specific experimental values are difficult to isolate in this plot, but the calculated data should closely fit the lines $u^+ = 2.5 \ln y^+ + 5$ and $T^+ = 2.5 \ln y^+ + 1$. Local wall temperatures and the average friction velocity were used to calculate T^+. The slope of the logarithmic profile depends on the wall heat flux. An error of ☐ 2% in the heat flux changes the slope by approximately ☐0.05.

Star-CCM+ and Solid Works Model:

The model was built in Sold Works using the data provided by Baglietto and the paper by Meyer. The model has thirty degree symmetry since it is a triangular rod array. This means that all the boundary conditions can be symmetry or adiabatic except for the imposed heat flux or heat source condition. The full model used in the Star-CCM+ calculations is shown in Figure 4.5. The sub-models are shown in Figure 4.6 for the heat flux on the fluid face and the heat source in the Model.

The boundary conditions for the model were an inlet velocity of 22.7 m/s and a pressure outlet condition. The inlet/outlet temperatures were set to 294 K as well as the initial conditions.

The first Star-CCM+ model similar to the STAR-CD one used by Baglietto with the 1.37 W/m^2 heat flux on the inside of the fluid did not give results that were comparable to Baglietto's results.

The second model shown in Figure 4.6 with the energy as a heat source did give very comparable results. The mesh is shown in Figure 4.7. Two calculations were performed for a mesh of ~ 50 K polyhedrons and prism layers and another with ~ 300 K polyhedrons, prism layers and thin mesh layers as shown in Figure 4.8. The prisms were used in the fluid for boundary layers and the thin mesher regions for the Monel.

The model was run with the attached settings for Star-CCM+, "Anisotropic Setup for Starccm+".

Analytical solutions or approximations:

Not available.

Validation database:

The experiment is described in:

"Measurements of turbulent velocity and temperature in axial flow through a heated rod bundle", L. Meyer, *Nuclear Engineering and Design* 146, pp 71-82, 1994.

References:

[4.1] "Anisotropic Turbulence Modeling for Accurate Rod Bundle Simulations", E. Baglietto, ICONE14-89646, July 2006.

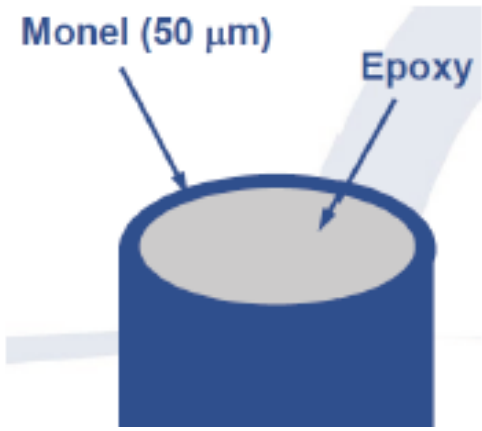

Figure 4.2 Rod composition

Table 4.1 Material Properties

Material	*Rho [kg/m³]*	*K [W/mK]*	*Others*
Air	1.08554	0.0281674	Mu 1.94113e-5 kg/ms
Monel	8830	20	Cp 427 (unnecessary)
Epoxy	1149	0.75	Cp 1883 (unnecessary)

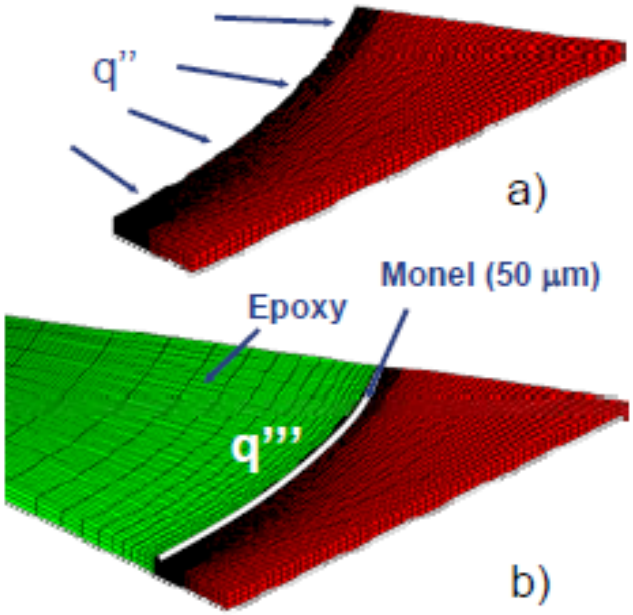

Figure 3

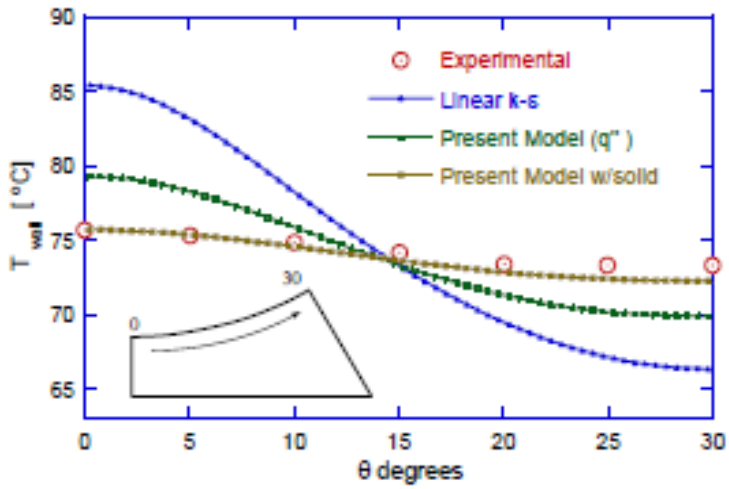

Figure 4

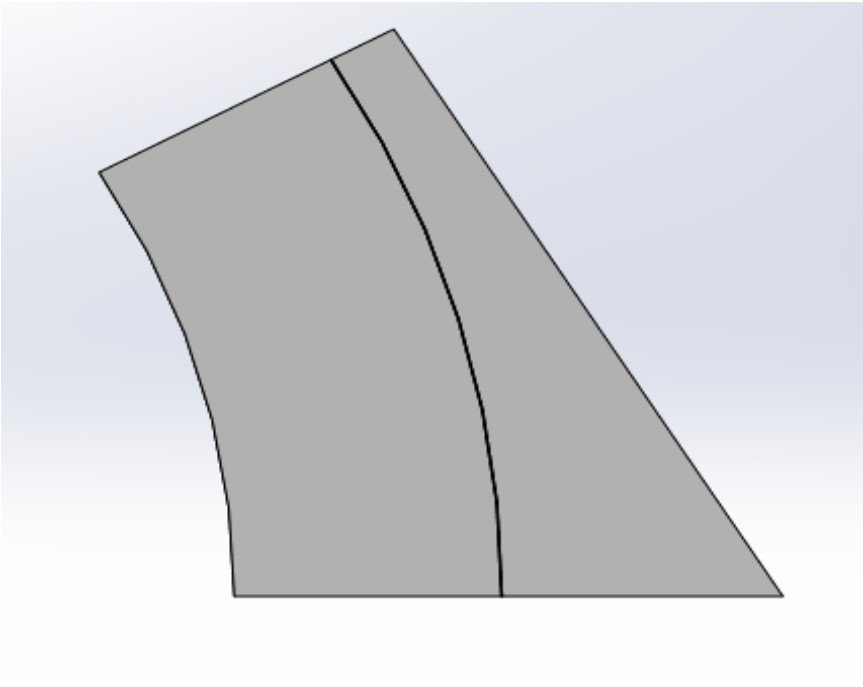

Figure 5

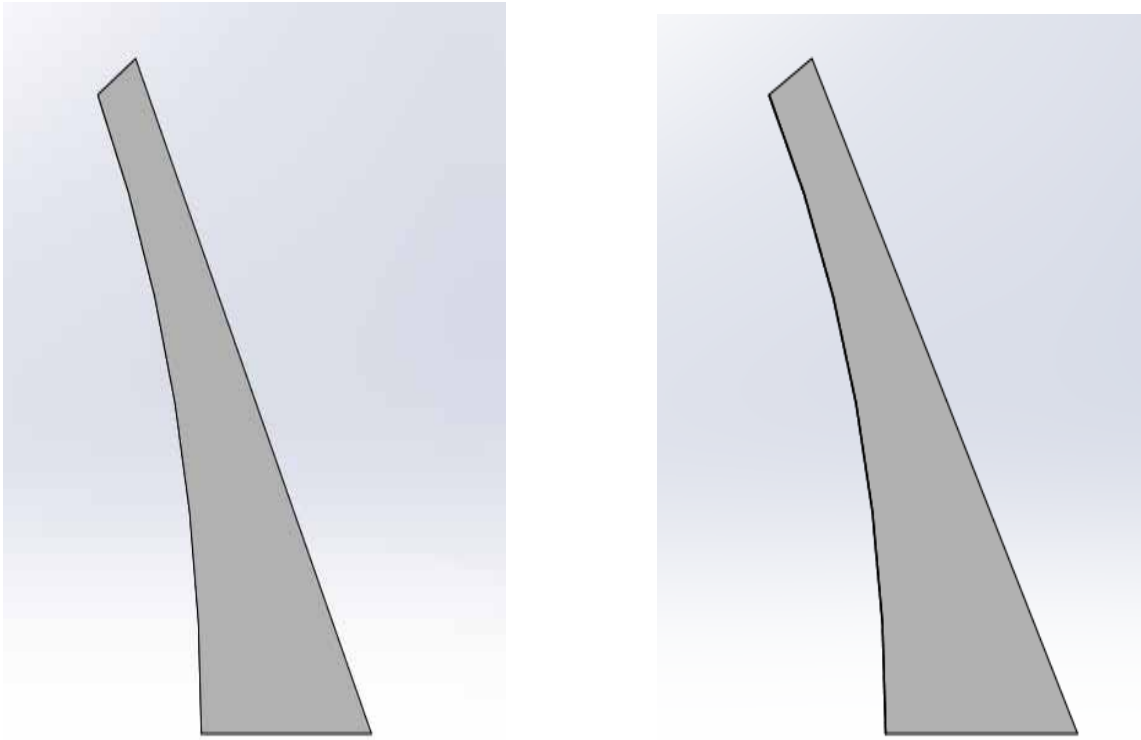

Figure 6

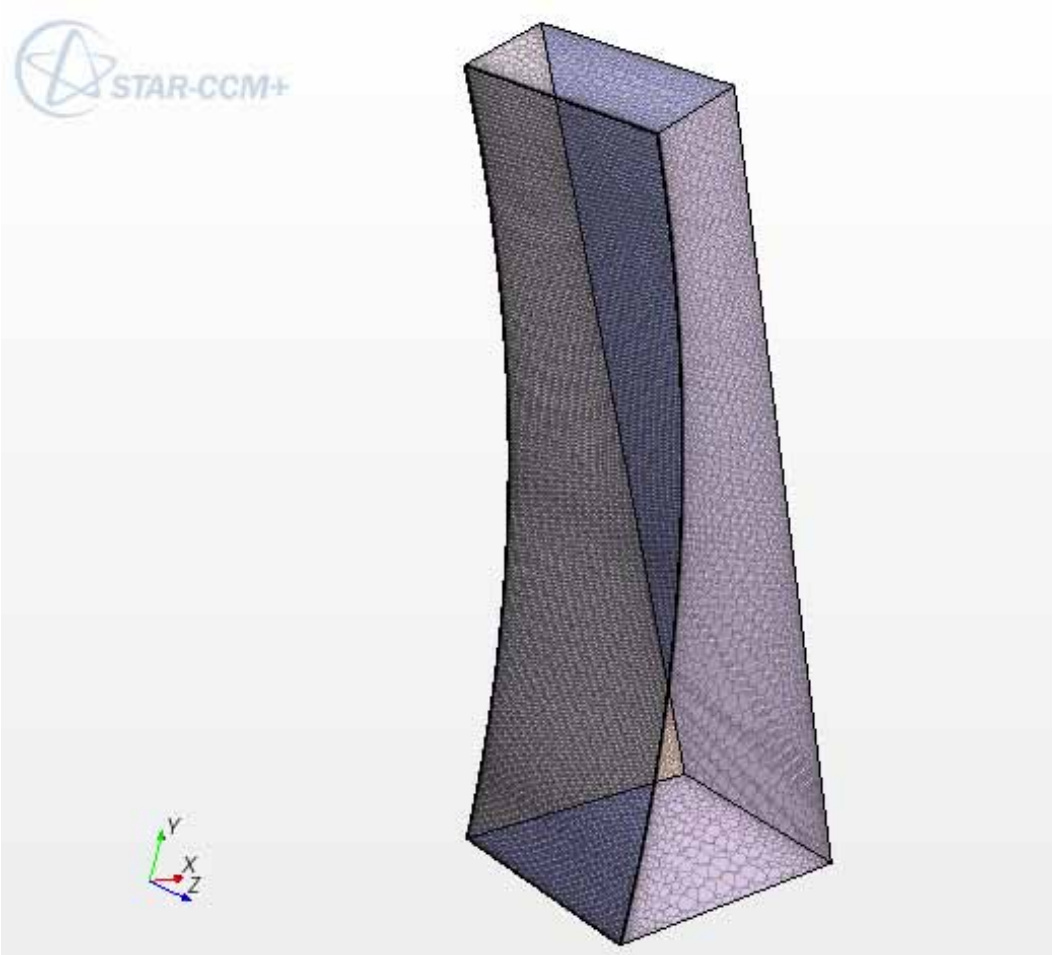

Figure 7

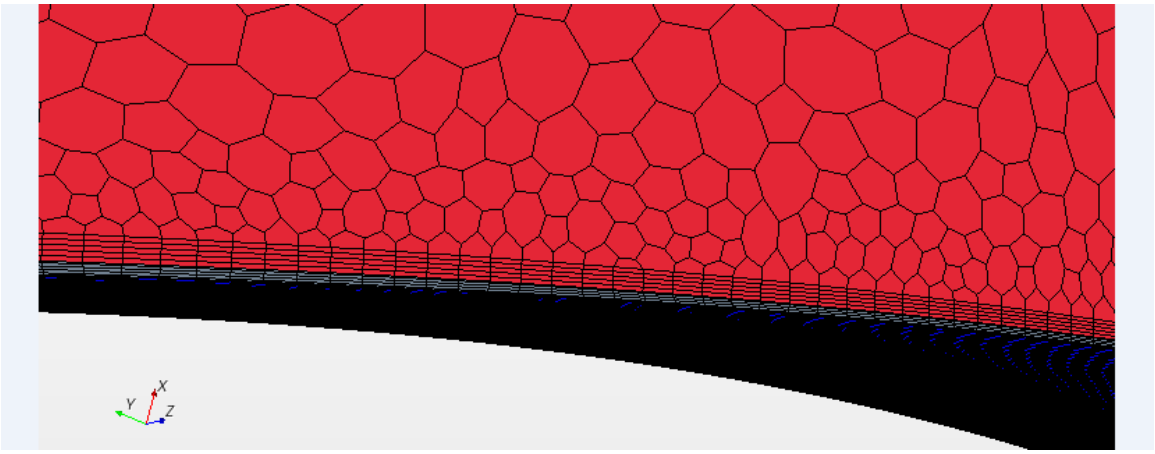

Figure 8

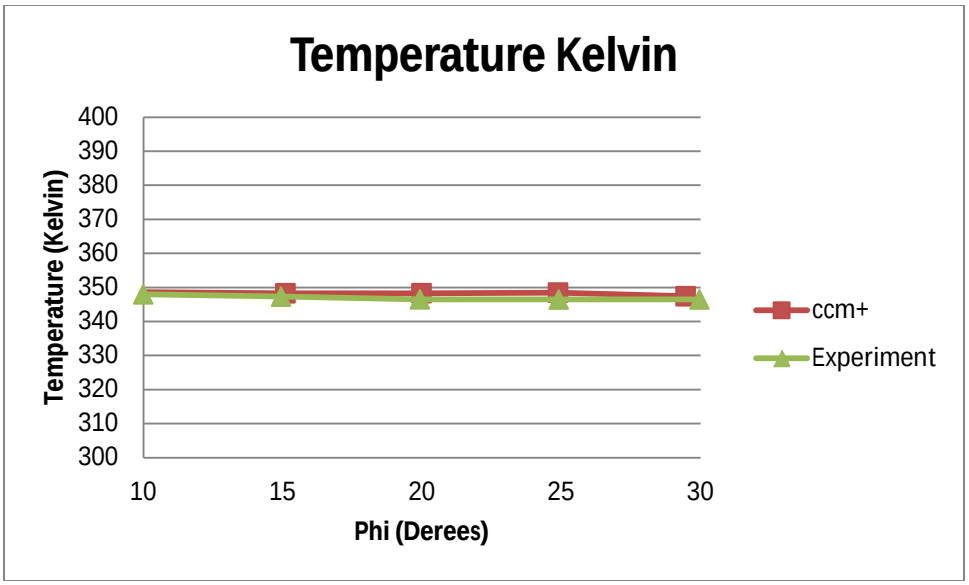

Figure 9 Comparisons of Star-CCM+ Model and Data